

Generalized Collective Inference with Symmetric Clique Potentials

Rahul Gupta Sunita Sarawagi Ajit A. Dewan
{grahul,sunita,aad}@cse.iitb.ac.in
Indian Institute of Technology, Bombay, India

Abstract

Many tasks like image segmentation, web page classification, and information extraction can be cast as joint inference tasks in collective graphical models. Such models exploit any inter-instance associative dependence to output more accurate labelings. However existing collective models support very limited kind of associativity — like associative labeling of different occurrences of the same word in a text corpus. This restricts accuracy gains from using such models.

In this work we make two major contributions. First, we propose a more general collective inference framework that encourages various data instances to agree on a set of *properties* of their labelings. Agreement is encouraged through symmetric clique potential functions. We show that known collective models are specific instantiations of our framework with certain very simple properties. We demonstrate that using non-trivial properties can lead to bigger gains, and present a systematic inference procedure in our framework for a large class of such properties. In our inference procedure, we perform message passing on the cluster graph, where property-aware messages are computed with cluster specific algorithms. Ordinary property-oblivious message passing schemes are intractable in such setups. We show that property conformance, as encouraged in our framework, provides an inference-only solution for domain adaptation. Our experiments on bibliographic information extraction illustrate significant test error reduction over unseen domains.

Our second major contribution is a suite of algorithms to compute messages from clique clusters to other clusters for a variety of symmetric clique potentials (the *clique inference* problem). Our algorithms are exact for arbitrary cardinality-based clique potentials on binary labels and for max-like and majority-like clique potentials on multiple labels. For majority-like potentials, we also provide an efficient Lagrangian Relaxation based algorithm that compares favorably with the exact algorithm. Moving towards more complex potentials, we show that clique inference becomes NP-hard for cliques with homogeneous Potts potentials. We present a $\frac{13}{15}$ -approximation algorithm with runtime sub-quadratic in the clique size. In contrast, the best known previous guarantee for graphs with Potts potentials is only $\frac{1}{2}$. We perform empirical comparisons on real and synthetic data, and show that our proposed methods for Potts potentials are an order of magnitude faster than the well-known Tree-based re-parameterization (TRW) and graph-cut algorithms. We demonstrate that our Lagrangian Relaxation based algorithm for majority potentials beats the best applicable heuristic, ICM, in a variety of scenarios.

1 Introduction

A variety of structured tasks such as image segmentation, information extraction, part of speech tagging, text chunking, and named entity recognition are modeled using Markov Random Fields (MRFs). For example, in information extraction, each sentence is treated as a MRF that captures the dependency in the labels assigned to adjacent words in the sentence.

An example of such a setup is given in Figure 1 for the task of named-entity extraction (NER). The base model in Figure 1(b) assigns a named-entity label such as Person, Location, or Other independently to each word in the input. The structured model goes one step ahead and imposes a dependency between labels of adjacent words, shown in Figure 1(c) via chain-shaped MRF models. The model, however, ignores long range and inter-sentence dependencies. The collective model of Figure 1(d) encourages the labels of different occurrences of the same word to be the same. This is captured by connecting those occurrences with blue cliques that encode associative dependencies. Variants of these collective models have been proposed in the past few years for a variety of information extraction tasks [22, 6, 15, 9, 10]. We look at other applications of collective graphical models in Section 2.

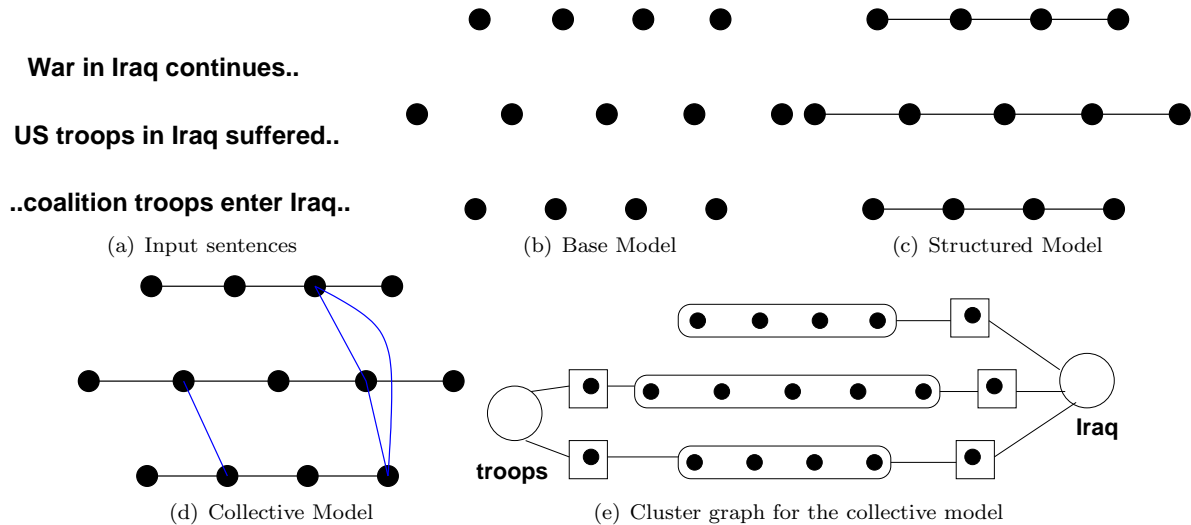


Figure 1: Various models for named-entity recognition illustrated on a small corpus. In Figure 1(e) the boxes denote separators that link the clusters. The 'size' of a separator is the number of nodes inside it.

Model	Scoring function	Inference algorithm	Complexity
Base	$\sum_{\text{chain } h} \sum_{u \in h} \phi_u(\mathbf{x}, y_u)$	$\text{argmax}_{y_u} \phi_u(\mathbf{x}, y_u)$ for each vertex u independently (Exact inference)	$ Y $ per vertex
Structured	Base + $\sum_h \sum_{(u,v) \in h} \phi_{uv}(\mathbf{x}, y_u, y_v)$	Max-product separately on each chain (Exact)	$O(V Y ^2)$ per chain
Collective	Structured + $\sum_{\text{clique } c} \phi_c(y_c)$	Message passing on the cluster graph (Approximate)	$O(Y ^{\text{biggest separator}})$ per cluster

Table 1: A brief summary of various graphical models for information extraction.

The key ingredient in a collective model is the set of potentials used to tie the individual MRFs together. These potentials, which can be defined over cliques of arbitrary size, encourage their vertices to have the same/similar label. We consider a special kind of clique potentials — symmetric potentials. Symmetric clique potentials are invariant under any permutation of their arguments. This restriction is meant to keep inference tractable with such potentials. Collective inference uses symmetric potentials that encourage all the vertices to take the same label. This can be enforced by choosing an appropriate bias function in the potential. Various kinds of symmetric potentials have been used in collective inference thus far — e.g. Potts potentials [22, 5] and Majority potentials [15]. We look at various families of symmetric clique potentials in Section 3.

Properties-based Collective Inference Framework

Figure 1 illustrates a highly common collective model in literature. Such a model enforces a very special kind of associativity — that labels of repeated occurrences of a word should be the same. Restricting ourselves to such collective models does not allow us to exploit the full power of collective inference, especially when unexploited associativity of a more complex nature exists in the data, e.g. all occurrences of Person should be preceded by titular tokens such as Mr. or Mrs. We broaden the notion of collective inference to encourage for richer forms of associativity amongst the labelings of multiple MRFs. This more general framework has applications in domain

adaptation. We illustrate this via an example.

Example: Consider extracting bibliographic information from an author’s publications homepage using a model trained on a different set of authors. Typically, within each home (a domain) we expect consistency in the style of individual publication records. For example, we expect that labelings of individual bibliographic records (approximately) use the same ordering of labels (say $Title \rightarrow Author^* \rightarrow Venue$), regardless of what that ordering is. Another property whose conformance might be desirable is — ”the HTML tag containing the Title of the publication”. Different bibliographic records on the same page will most probably format the title using the same HTML tag. Thus, we can encode this associativity by biasing the labelings to be conformant wrt this property. For both these properties, we only demand that the labelings agree on the property value, without caring for what the value actually is (which varies from domain to domain). This allows us to use the same property on different domains, with varying formatting and authoring styles.

Now assume that we have an array of such conformance-promoting properties, and a sequential chain model trained on a set of labeled domains. We show that an effective way of adapting the trained model to a new domain is by labeling the MRFs in the new domain collectively while encouraging the individual labelings to agree on our set of properties. This is an inference-only approach, unlike many existing solutions for domain adaptation which require expensive model re-training [1, 2, 17]. As we will see in Section 7.2, using this properties-based framework provides significant gains on a bibliographic information extraction task.

To summarize, our collective inference framework consists of two new components attached to any collection of MRFs:

- Properties: defined over the labelings of individual MRFs,
- Potentials: defined on the values of properties of all MRFs such that the potential value favors skewness in the frequencies of property values.

We describe our framework in detail in Section 4.

The collective inference task in our framework is to choose a labeling of the individual MRFs so as to maximize the sum of the scores of each MRF and the potentials of each property. This inference task is more complicated than independently labeling each MRF, which are typically simple tractable models like sequences.

We address the computational challenge by defining special forms of decomposable properties and symmetric potentials that allow efficient inference without sacrificing usability. We exploit this special structure to design efficient MAP inference algorithms. Instead of ordinary belief propagation on the joint graphical model, we define a cluster graph with two kinds of clusters — corresponding to tractable MRFs, and cliques with symmetric potential functions. Two important aspects of this algorithm are as follows. First, we use combinatorial methods to compute cluster-specific messages. In Section 6 we present exact and approximate clique inference algorithms for a variety of symmetric potential functions. These algorithms are used to compute max-marginal messages from a clique to its neighboring clusters. Second, we exploit the form of our properties to define new intermediate message variables, and provide exact and approximate algorithms for computing these special message values in Section 5. In contrast, a naïve application of graphical model inference could lead to an entire MRF instance being a separator.

In Section 7 our experiments on real tasks show that this form of message passing is faster and more accurate than existing inference methods that do not exploit the form of the potentials.

Finally in Section 8, we discuss some future directions for collective inference and outline some important problems in the area.

Contributions

Our first key contribution is a framework that encourages associativity between properties of labelings of isolated MRFs. We show that the framework support a large class of *decomposable* properties. Our properties are functions of a data-instance and its labeling, in contrast to the existing associative setups which model only very specific properties of only the instances. We give an approximate inference procedure based on message passing on the cluster graph, for computing the MAP labeling in our framework. Our procedure maintains tractability by computing property-aware messages and invoking special combinatorial algorithms at the cliques.

The second key contribution is a family of algorithms for various kinds of symmetric clique potential functions. We give an $O(mn \log n)$ MAP algorithm for cliques with arbitrary symmetric potentials, where m is the number

of labels, and n is the clique size. This algorithm is exact for max-like potentials, and is $\frac{13}{15}$ -approximate for Potts potentials. We show that this algorithm can be generalized to an $O(m^2n \log n)$ algorithm while improving the approximation bound to $\frac{8}{9}$. For majority-like potentials, we present an LP-based exact algorithm with polynomial but expensive runtime. We present an alternative approximate algorithm based on Lagrangian relaxation that is two orders of magnitude faster and provides close to optimal quality solutions in practice.

Finally, we show that our suite of algorithms can be plugged into the properties-based framework to achieve a highly expressive way for capturing associativity. We illustrate this on a bibliographic information task where we use properties to deploy our collective framework over unseen bibliographic domains, and achieve significant error reductions.

Outline

In Section 2, we give some real-life scenarios where collective inference can be used to exploit associativity amongst isolated MRF instances. We model associativity using symmetric potentials. In Section 3, we describe three families of symmetric potentials, that subsume the Potts and linear MAJORITY potentials. Section 4 discusses our properties-based collective inference framework in formal detail. Our framework ensures tractability of inference as long as the properties are *decomposable*, a notion that we cover in Section 4.1. In Section 5, we discuss the cluster message passing algorithm to compute the MAP in our framework. Section 5.1 presents our approach for exactly computing property-aware messages from an MRF instance to a clique, and Section 5.1.2 contains practical approximations of this exact computation. In Section 5.2, we show that computing the reverse message – from a clique to a MRF instance, is the same as the *clique inference problem*. Then in Section 6, we present algorithms for solving the clique inference problem under a variety of symmetric clique potentials. The two key algorithms presented are the α -pass algorithm and a Lagrangian-relaxation based algorithm for MAJORITY potentials, in Sections 6.1 and 6.3.3 respectively. Section 7 contains experimental results of three types – (a) Establishing that our properties based framework leads to significant gains in a domain adaptation task. (b) Our clique inference algorithms are better than applicable alternatives and (c) The cluster message passing framework is a better way of doing inference. Finally, Section 8 contains conclusions and a discussion of future work.

2 Applications of Collective Inference

We review a few practical applications of collective inference in real-life tasks. Both the tasks benefit when we introduce associative dependencies between labelings of isolated instances.

2.1 Information Extraction

Recall Figure 1(d) for the task of named-entity extraction. Let the potential function for an edge between adjacent word positions $j - 1$ and j in document i be $\phi_{ij}(y, y')$ and for non-adjacent positions that share a word w be $f_w(y, y')$. The goal during inference is to find a labeling \mathbf{y} where y_{ij} is the label of word x_{ij} in position j of doc i , so as to maximize:

$$\sum_{i,j} \phi_{ij}(y_{ij}, y_{i(j-1)}) + \sum_w \sum_{x_{ij}=x_{i'j'}=w} f_w(y_{ij}, y_{i'j'}) \quad (1)$$

The above inference problem gets intractable very soon with the addition of non-adjacent edges beyond the highly tractable collection of chain models of classical IE. Consequently, all prior work on collective extraction for IE relied on generic approximation techniques including belief propagation [22, 6], Gibbs sampling [9] or stacking [15].

We present a different view of the above inference problem using cardinality-based clique potential functions $C_w(\cdot)$ defined over label subsets \mathbf{y}^w of positions where word w occurs. We rewrite the second term in Equation 1 as

$$\begin{aligned} \frac{1}{2} \sum_w \left(\sum_{y,y'} f_w(y, y') n_y(\mathbf{y}^w) n_{y'}(\mathbf{y}^w) - \sum_y n_y(\mathbf{y}^w) f_w(y, y) \right) \\ = \sum_w C_w(n_1(\mathbf{y}^w), \dots, n_m(\mathbf{y}^w)) \end{aligned}$$

where $n_y(\mathbf{y}^w)$ is the number of times w is labeled y in all its occurrences. The clique potential C_w only depends on the counts of how many nodes get assigned a particular label. A useful special case of the function is when $f_w(y, y')$ is positive only for the case that $y = y'$, and zero otherwise.

2.2 Hypertext classification

In hypertext classification, the goal is to classify a document based on features derived from its content and labels of documents it points to. A common technique in statistical relational learning to capture the dependency between a node and the variable number of neighbors it might be related to, is to define fixed length feature vectors out of the neighbor’s labels. In text classification, most previous approaches [24, 16, 7] have created features based on the counts of labels in its neighborhood. Accordingly, we can define the following set of potentials: a node-level potential $\phi_i(y)$ that depends on the content of the document i , and a neighborhood potential $f(y, n_1(\mathbf{y}^{O_i}), \dots, n_m(\mathbf{y}^{O_i}))$ that captures the dependency of the label of i on the counts in the label vector \mathbf{y}^{O_i} of its out-links.

$$\begin{aligned} & \sum_i (\phi_{iy_i} + f(y_i, n_1(\mathbf{y}^{O_i}), \dots, n_m(\mathbf{y}^{O_i}))) \\ = & \sum_i (\phi_{iy_i} + \sum_y C_y(n_1(\mathbf{y}^{O_i}), \dots, n_m(\mathbf{y}^{O_i})) \mathbb{I}[y = y_i]) \end{aligned}$$

[16] include several examples of such clique potentials, viz. the Majority potential $C_y(n_1, \dots, n_m) = \phi(y, y_{max})$ where $y_{max} = \operatorname{argmax}_y n_y$, and the Count potential $C_y(n_1, \dots, n_m) = \sum_{y': n_{y'} > 0} \phi(y', y) n_{y'}$. Some of these potentials, for example, the Majority potential are not decomposable as sum of potentials over the edges of the clique. This implies that methods such as TRW and graph-cuts are not applicable. [16] rely on the Iterated Conditional Modes (ICM) method that greedily selects the best label of each document in turn based on the label counts of its neighbors.

3 Symmetric Clique Potentials

As seen in the example scenarios, our associative clique potentials depend only on the number of clique vertices taking a value v , denoted by n_v , and not on the identity of those vertices. In other words, these potentials are invariant under any permutation of their arguments and derive their value from the histogram of counts $\{n_v | \forall v\}$. We denote this histogram by the vector \mathbf{n} . Since the potentials only depend on the value counts, we also refer to them as cardinality-based clique potentials in this paper. If a cardinality-based clique potential is associative, then it is maximized when $n_v = n$ for some v , i.e. one value is given to all the clique vertices.

We have deliberately left the notion of a ‘value’ vague at this point. For existing collective models, e.g. those mentioned in Section 2, a value corresponds to a label. As we shall see, in our more general framework, a value refers to a particular member in the range of a property function. For now, we can assume wlog that a *value* is a member of some discrete finite set V .

We consider specific families of clique potentials, many of which are currently used in real-life tasks. In Section 6 we will look at various potential-specific exact and approximate clique inference algorithms that exploit the specific structure of the potential.

In particular, we consider the three types of clique potentials listed in Table 2.

3.1 MAX clique potentials

These clique potentials are of the form:

$$C(n_1, \dots, n_{|V|}) = \max_v f_v(n_v) \tag{2}$$

for arbitrary non-decreasing functions f_v . When $f_v(n_v) \triangleq n_v$, we get the *makespan* clique potential which has roots in the job-scheduling literature.

In Section 6.1, we present an algorithm, called α -pass, that solves the clique inference problem for MAX potentials exactly. The algorithm runs in time $O(|V|n \log n)$, where n is the clique size, Although MAX potentials

Name	Form	Remarks
MAX	$\max_v f_v(n_v)$	f_v is a non-decreasing function
SUM	$\sum_v f_v(n_v)$	f_v non-decreasing. Includes the Potts potential = $\lambda \sum_v n_v^2$
MAJORITY	$f_a(\mathbf{n})$, where $a = \operatorname{argmax}_v n_v$	f_a is typically linear

Table 2: Various kinds of symmetric clique potentials considered in this paper. $\mathbf{n} = (n_1, \dots, n_{|V|})$ denotes the counts of various values among the clique vertices.

are not used directly in real-life tasks, they are relatively easier potentials to tackle and provide key insights to deal with the more complex SUM potentials. As we will see, the α -pass algorithm that we derive for this potential can be easily ported to other more complex potentials. For the case of Potts potentials, we will prove that the α -pass algorithm provides a $\frac{13}{15}$ -approximation.

3.2 SUM clique potentials

SUM clique potentials are of the form:

$$C(n_1, \dots, n_{|V|}) = \sum_v f_v(n_v) \quad (3)$$

These form of potentials includes the special case when the well-known Potts model is applied homogeneously on all edges of a clique. Let λ be the Potts potential of assigning two nodes of an edge the same value. The summation of these potentials over a clique is equivalent (up to a constant) to the clique potential:

$$C^{\text{Potts}} = C(n_1, \dots, n_{|V|}) = \lambda \sum_v n_v^2 \quad (4)$$

The Potts model with negative λ corresponds to the dis-associative case when edges prefer the two end points to take different values. The more interesting case is when λ is positive. For this case, we will borrow the α -pass algorithm for MAX potentials and show that it gives a $\frac{13}{15}$ -approximation.

3.3 MAJORITY potentials

MAJORITY potentials have been used for a variety of tasks such as link-based classification of web-pages [16] and named-entity extraction [15]. A majority potential over a clique C is parameterized by a $|V| \times |V|$ matrix $W = \{w_{vv'}\}$. The role of W is to capture the co-existence of different value pairs in the same clique.

Co-existence allows us to downplay ‘strict associativity’ viz. giving all vertices of a clique the same value. The justification for co-existence is as follows. Consider the conventional collective inference model for named-entity recognition (Figure 1(d)) where a value corresponds to a label. Suppose the word ‘America’ occurs in a corpus multiple times. Then all occurrences of ‘America’ will be joined with an associative clique. However, some occurrences of America correspond to Location, while others might correspond to an Organization, say Bank of America. Thus we require most but not all vertices in the America clique to be labeled similarly. This motivates the need for a clique potential with scope for co-existence.

Coming back to W , a highly positive $w_{vv'}$ would suggest that the values v and v' should be allowed to co-exist in a clique, when v is the majority value in the clique. We allow $w_{vv'}$ to be negative to model mutual-exclusion amongst value pairs. Our algorithms work for unrestricted W , although in practice the training procedure that learns W might add some constraints.

We know define MAJORITY potentials as:

$$C(n_1, \dots, n_{|V|}) = f_a(\mathbf{n}), \quad a = \operatorname{argmax}_v n_v \quad (5)$$

We consider linear majority potentials where $f_a(\mathbf{n}) = \sum_v w_{av} n_v$. The matrix $W = \{w_{vv'}\}$ need not be diagonally dominant or even symmetric. Unlike Potts potential, MAJORITY potential cannot be represented using edge potentials.

4 Generalized Collective Inference Framework

We now discuss our framework for generalized collective inference. Recall that we wish to encourage the labelings of various isolated MRFs to agree on a set of properties. Our generalized collective inference framework consists of three parts:

1. A collection of structured instance-labeling pairs $\{(\mathbf{x}_i, \mathbf{y}_i)\}_{i=1}^N$ where each \mathbf{y}_i is probabilistically modeled using a corresponding Markov Random Field (MRF). Let $\phi(\mathbf{x}_i, \mathbf{y}_i)$ be a scoring function for assigning labeling \mathbf{y}_i to \mathbf{x}_i using the MRF. The scoring function decomposes over the parts c of the MRF as $\phi(\mathbf{x}_i, \mathbf{y}_i) = \sum_c \phi_c(\mathbf{x}_i, \mathbf{y}_c)$.
2. A set P of properties where each property $p \in P$ includes in its domain a subset \mathcal{D}_p of MRFs and maps each labeling \mathbf{y} of an input $\mathbf{x} \in \mathcal{D}_p$ to a discrete value from its range \mathcal{R}'_p . Each property decomposes over cliques of the MRF. We discuss decomposable properties in Section 4.1
3. A clique potential $C_p(\{p(\mathbf{x}_i, \mathbf{y}_i)\}_{\mathbf{x}_i \in \mathcal{D}_p})$ for each property p . This potential is a symmetric function of its input. We elaborated on various symmetric potential functions in Section 3. These potentials encourage conformity of properties across labelings of multiple MRFs.

The collective inference task is to label the N instances so as to maximize the sum of the individual MRF specific scores and the clique potentials coupling many MRFs via the property functions. This is given by:

$$\max_{(\mathbf{y}_1, \dots, \mathbf{y}_N)} \sum_{i=1}^N \phi(\mathbf{x}_i, \mathbf{y}_i) + \sum_{p \in P} C_p(\{p(\mathbf{x}_i, \mathbf{y}_i)\}_{i \in \mathcal{D}_p}) \quad (6)$$

Even for symmetric C_p and binary labels, Equation 6 is NP-hard to optimize. One well-known hard case is the Ising model, where each C_p is a Potts potential. Thus we look at an approximate approach based on message passing that we elaborate in Section 5.

4.1 Decomposable Properties

A property maps a (\mathbf{x}, \mathbf{y}) pair to a discrete value in its range. Typically, since \mathbf{y} is exponentially large in the size of \mathbf{x} , we cannot solve Equation 6 tractably without constructing the value of a property from smaller components of \mathbf{y} . We define *decomposable* properties as those which can be broken over the parts c of the MRF of labeling \mathbf{y} , just like ϕ . Such properties can be folded into the message computation steps at each of the MRFs, as we shall see in Section 5. We now formally describe decomposable properties:

Definition 4.1. A decomposable property $p(\mathbf{x}, \mathbf{y})$ is composed out of component level properties $p(\mathbf{x}, \mathbf{y}_c, c)$ defined over parts c of \mathbf{y} . $p : (\mathbf{x}, \mathbf{y}_c, c) \mapsto \mathcal{R}_p \cup \{\perp\}$ where the special symbol \perp means that the property is not applicable to $(\mathbf{x}, \mathbf{y}_c, c)$. $p(\mathbf{x}, \mathbf{y})$ is composed as:

$$p(\mathbf{x}, \mathbf{y}) \triangleq \begin{cases} \emptyset & \text{if } \forall c : p(\mathbf{x}, \mathbf{y}_c, c) = \perp \\ v & \text{if } \forall c : p(\mathbf{x}, \mathbf{y}_c, c) \in \{v, \perp\} \\ \perp & \text{otherwise.} \end{cases} \quad (7)$$

The first case occurs when the property does not fire over any of the parts. The last case occurs when \mathbf{y} has more than one parts where the property has a valid value but the values are different. The new range \mathcal{R}'_p now consists of \mathcal{R}_p and the two special symbols \perp and \emptyset .

We show that even with decomposable properties we can express many useful types of regularities in labeling multiple MRFs arising in applications like domain adaptation.

Example 1 We start with an example from the simple collective inference task of [22, 6, 9] of favoring the same label for repeated words. Let \mathbf{x} be a sentence and \mathbf{y} be a labeling of all the tokens of \mathbf{x} . Consider a property

p , called **TokenLabel**, which returns the label of a fixed token t . Then, \mathcal{D}_p comprises of all \mathbf{x} which have the token t , and \mathcal{R}_p is the set of all labels. Thus, if $\mathbf{x} \in \mathcal{D}_p$, then

$$p(\mathbf{x}, y_c, c) \triangleq \begin{cases} y_c & \mathbf{x}_c = t \\ \perp & \text{otherwise} \end{cases} \quad (8)$$

and, given \mathbf{y} and $\mathbf{x} \in \mathcal{D}_p$,

$$p(\mathbf{x}, \mathbf{y}) \triangleq \begin{cases} y & \text{all occurrences of } t \text{ in } \mathbf{x} \text{ are labeled with label } y \\ \perp & \text{otherwise} \end{cases} \quad (9)$$

Example 2 Next consider a more complex example that allows us to express regularity in the order of labels in a collection of bibliography records. Let \mathbf{x} be a publications record and \mathbf{y} its labeling. Define property p , called **NextLabel**, which returns the first non-Other label in \mathbf{y} after a Title. A special label ‘End’ marks the end of \mathbf{y} . So \mathcal{R}_p contains ‘End’ and all labels except Other. Thus,

$$p(\mathbf{x}, y_c, c) \triangleq \begin{cases} \beta & y_c = \text{Title} \wedge y_{c+i} = \beta \wedge (\forall j : 0 < j < i : y_{c+j} = \text{Other}) \\ \text{End} & y_c = \text{Title} \wedge c \text{ is the last clique in } \mathbf{y} \\ \perp & y_c \neq \text{Title} \end{cases} \quad (10)$$

Therefore,

$$p(\mathbf{x}, \mathbf{y}) \triangleq \begin{cases} \emptyset & \mathbf{y} \text{ has no Title} \\ \beta & \beta \text{ is the first non-Other label following } \mathbf{each} \text{ Title in } \mathbf{y} \\ \perp & \text{otherwise} \end{cases} \quad (11)$$

Example 3 In both the above examples the range \mathcal{R}'_p of the properties was labels. Consider a third property, called **BeforeToken** whose range is the space of tokens. This property returns the identity of the token before a Title in \mathbf{y} . So,

$$p(\mathbf{x}, y_c, c) \triangleq \begin{cases} x_{c-1} & y_c = \text{Title} \wedge (c > 0) \\ \text{‘Start’} & y_c = \text{Title} \wedge (c = 0) \\ \perp & y_c \neq \text{Title} \end{cases} \quad (12)$$

Therefore,

$$p(\mathbf{x}, \mathbf{y}) \triangleq \begin{cases} \emptyset & \text{No Title in } \mathbf{y} \\ \text{‘Start’} & \text{The only Title in } \mathbf{y} \text{ is at the beginning of } \mathbf{y} \\ t & \text{All Titles in } \mathbf{y} \text{ are preceded by token } t \\ \perp & \mathbf{y} \text{ has two or more Titles with different preceding tokens} \end{cases} \quad (13)$$

Some important families of symmetric clique potentials have been described in [10], and recalled in Section 3. We use two most widely used of those families, called Potts and MAJORITY, defined as:

$$\begin{aligned} C^{\text{Potts}}(\{v_1, \dots, v_n\}) &\triangleq \lambda \sum_{v'} n_{v'}^2 \\ C^{\text{Maj}}(\{v_1, \dots, v_n\}) &\triangleq \sum_{v'} w_{\hat{v}v'} n_{v'}, \quad \hat{v} = \operatorname{argmax}_v n_v \end{aligned}$$

where n_v is frequency of v in the multiset $\{v_1, \dots, v_n\}$ and λ, w are fixed parameters of the potentials.

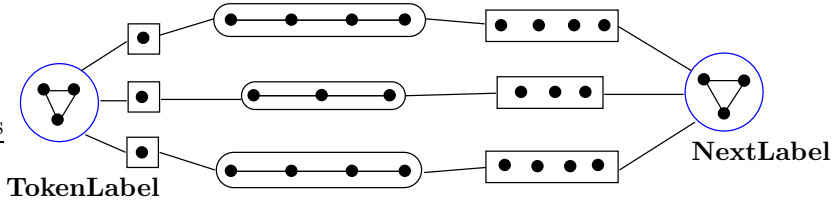


Figure 2: Cluster graph for a toy example with three chain-shaped MRF instances and two properties. The **TokenLabel** property has thin separators, while **NextLabel** has separators that consist of the entire instance. Both the properties have associative potentials defined on their cliques (shown as blue circles).

5 MAP Estimation in the Generalized Collective Inference Framework

The natural choice for approximating the NP-hard objective in Equation 6 is ordinary pairwise belief propagation on the joint model. This approach does not work due to many reasons. First, some symmetric potentials like the MAJORITY potential cannot be decomposed along the edges. Second, property-aware messages cannot be computed for arbitrary message passing schedules. Third, cluster-membership information of vertices, which is very vital, is not exploited at all.

Other approaches like the stacking based approach of [15] are specific to particular symmetric potentials and do not exploit the full set of messages to compute a more accurate MAP.

Hence we adopt message passing on the cluster graph of the model as our approach, akin to the one proposed by [8]. We create a top-level cluster graph model where the clusters correspond to the N instances and $|P|$ property cliques. The cluster node of each instance is internally another nested MRF. The cluster for a property p is a clique whose vertices correspond to instances in \mathcal{D}_p . Figure 2 illustrates an example with two properties and three data instances.

For complex properties like the **NextLabel** property of Section 4.1, the separator between a MRF cluster and a property cluster is the entire instance. This is a major departure from known collective models such as the one in Figure 1(e). Known collective models use highly simple properties, e.g. **TokenLabel** in Figure 1(e), which lead to single vertex separators because the property clique is incident on instances only through a single token, which is known in advance. In the case of complex properties like **NextLabel**, not only is the property clique incidence information missing, but the clique’s incidence is dependent on the property of the entire labeling and not just a single token’s label. This causes the entire instance to be a separator between the property cluster and the instance MRF cluster. Therefore, naïve message passing schemes whose runtime is exponential in the separator size are inapplicable here. However we exploit the decomposability of properties to simplify message updates.

The setup of message passing on the cluster graph allows us to exploit potential-specific algorithms at the cliques, and at the same time work with any arbitrary clique potential. It also allows intuitive computation of property-aware messages.

Let $m_{i \rightarrow p}$ and $m_{p \rightarrow i}$ denote message vectors from instance i to an incident property clique p and vice-versa. Let $v \in \mathcal{R}'_p$ denote a property value. Next we discuss how these messages are computed.

5.1 Message from an Instance to a Clique

The message $m_{i \rightarrow p}(v)$ is given by:

$$m_{i \rightarrow p}(v) = \max_{\mathbf{y}: p(\mathbf{x}_i, \mathbf{y})=v} \left(\phi(\mathbf{x}_i, \mathbf{y}) + \sum_{\substack{p' \neq p: \\ \mathbf{x}_i \in \mathcal{D}_{p'}}} m_{p' \rightarrow i}(p'(\mathbf{x}_i, \mathbf{y})) \right) \quad (14)$$

To compute $m_{i \rightarrow p}(v)$, we need to absorb the incoming messages from other incident properties $p' \neq p$, and do the maximization. When a property p' is applicable to only a single fixed clique c of the instance, we can easily

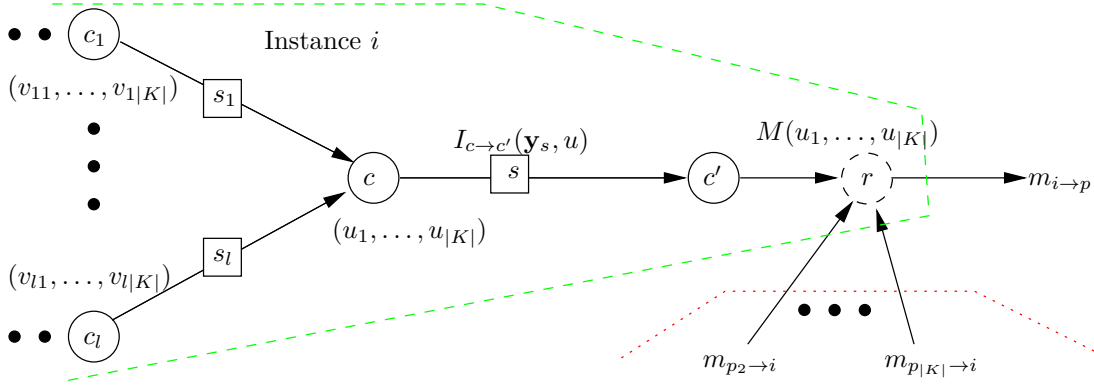


Figure 3: Computation of the message $m_{i \rightarrow p}$. Instance i is incident to $|K|$ properties $p_1, \dots, p_{|K|}$ where $p = p_1$. The green portion shows the internal messages $I(\cdot)$ in instance i . Final message $m_{i \rightarrow p}$ is computed in terms of the aggregated message $M(u_1, \dots, u_{|K|})$ and any incoming messages $m_{p_j \rightarrow i}$, $j > 1$ (the red portion).

absorb the message $m_{p' \rightarrow i}$ by including it in the potential of the clique, ϕ_c . This is true, for instance, for the TokenLabel property in the previous section when within a sentence the word does not repeat. In the general case, absorbing messages that are applicable over multiple cliques requires us to ensure that the cliques agree on the property values following Equation 7. We will refer to these as multi-clique properties.

We first present an exact extension of the message passing algorithm within an instance MRF to enforce such agreement and later present approximations. Let K be the set of multi-clique properties in whose domain instance \mathbf{x}_i lies. We are targeting applications where K is small.

5.1.1 Exact Messages

Figure 3 shows the various messages involved in computing the message $m_{i \rightarrow p}$. We describe the procedure step-by-step. Consider an internal message $I_{c \rightarrow c'}(\mathbf{y}_s)$ between adjacent cliques c and c' inside the MRF of instance i with s as the separator. This is computed in standard message passing as follows:

$$I_{c \rightarrow c'}(\mathbf{y}_s) = \max_{\mathbf{y}_c \sim \mathbf{y}_s} \phi_c(\mathbf{y}_c) + \sum_{j=1}^l I_{c_j \rightarrow c}(\mathbf{y}_{s_j}) \quad (15)$$

where $c_1 \dots c_l$ denote the l neighboring cliques of clique c excluding c' and $s_1 \dots s_l$ are the corresponding separators. To handle multi-clique properties, we augment these internal messages to maintain state about the set of properties already encountered in any partial labeling up to c .

For ease of explanation, first consider the case where $|K| = 1$, and let p be the only property relevant for instance i . We maintain messages of the kind $I_{c \rightarrow c'}(\mathbf{y}_s, u)$, where $u \in \mathcal{R}'_p$ is called the *value argument* of I . These messages compute the following quantity: what is the score of the best partial labeling \mathbf{y}_{part} up to c , which is consistent with \mathbf{y}_s , such that $p(\mathbf{x}, \mathbf{y}_{part}) = u$ (as per Definition 4.1) if we ignore the cliques beyond c' . To compute this message, we consider only the following entities:

1. All local labelings \mathbf{y}_c , consistent with \mathbf{y}_s , such that $p(\mathbf{x}, \mathbf{y}_c, c)$ does not conflict with u .
2. Incoming messages at c (except from c') of the kind $I_{c_i \rightarrow c}(\mathbf{y}_{s_i}, v_i)$ such that v_i does not conflict with u , and all the v_i 's together with $p(\mathbf{x}, \mathbf{y}_c, c)$ can produce a property value u at c .

Another way to look at it is as follows. Consider the green portion of Figure 3, and let v_1, \dots, v_l be l candidate property values produced by some partial labelings running up to c_1, \dots, c_l respectively. Also consider a local labeling \mathbf{y}_c at c , consistent with \mathbf{y}_s . Then computing the message $I_{c \rightarrow c'}(\mathbf{y}_s, u)$ is the same as *composing* u by picking a combination of \mathbf{y}_c and v_1, \dots, v_l such that $p(\mathbf{x}, \mathbf{y}_c, c), v_1, \dots, v_l$ can be amalgamated into u via Definition 4.1. If no such combination exists, then the message is $-\infty$, else we return the combination with the highest total score.

Thus, depending on u , Equation 15 is modified as follows:

Case 1: $u = \emptyset$: To get a value of \emptyset , the property should fire neither at c , nor up to or at any of the c_i 's. That is, we need $p(\mathbf{x}, \mathbf{y}_c, c) = \emptyset$ and incoming messages at c whose value arguments are also \emptyset . Thus $I_{c \rightarrow c'}(\mathbf{y}_s, \emptyset)$ is computed as:

$$\max_{\substack{\mathbf{y}_c \sim \mathbf{y}_s \\ p(\mathbf{x}, \mathbf{y}_c, c) = \perp}} \phi_c(\mathbf{y}_c) + \sum_{j=1}^l I_{c_j \rightarrow c}(\mathbf{y}_{s_j}, \emptyset)$$

Case 2: $u \in \mathcal{R}_p$: In this case, $p(\mathbf{x}, \mathbf{y}_c, c)$ the value arguments of its incoming messages should be one of u and \emptyset , with at least one of them being u (otherwise all of them will be \emptyset and we will get \emptyset at c). This will hold if the predicate $V_1(\mathbf{y}_c, v_1, \dots, v_l)$, defined below, is true.

$$V_1(\mathbf{y}_c, v_1, \dots, v_l) \triangleq (\forall j : v_j \in \{u, \emptyset\}) \wedge (p(\mathbf{x}, \mathbf{y}_c, c) \in \{u, \perp\}) \wedge (p(\mathbf{x}, \mathbf{y}_c, c) = u \vee \exists v_j = u) \quad (16)$$

Here v_1, \dots, v_l denote value arguments of the incoming messages at c excluding the one from c' . If the set $\{v_1, \dots, v_l, p(\mathbf{x}, \mathbf{y}_c, c)\}$ contains two distinct values from \mathcal{R}_p , then they will conflict and create \perp at c on composition. Thus, V_1 precisely and completely represents the set of valid combinations for producing u . Using V_1 we can compute $I_{c \rightarrow c'}(\mathbf{y}_s, u)$ as:

$$\max_{\substack{\mathbf{y}_c \sim \mathbf{y}_s, v_1, \dots, v_l \\ V_1(\mathbf{y}_c, v_1, \dots, v_l)}} \phi_c(\mathbf{y}_c) + \sum_{j=1}^l I_{c_j \rightarrow c}(\mathbf{y}_{s_j}, v_j) \quad (17)$$

Case 3: $u = \perp$: We can produce \perp when either (a) value arguments of two or more incoming messages at c conflict or (b) the property value at c conflicts with the value argument of one of the incoming messages or (c) either the property value at c or any one of the value arguments is \perp . The predicate $V_2(\mathbf{y}_c, v_1, \dots, v_l)$ returns true if any one of the above outcomes hold:

$$\begin{aligned} V_2(\mathbf{y}_c, v_1, \dots, v_l) &= (\exists j : v_j = \perp) \vee (p(\mathbf{x}, \mathbf{y}_c, c) = \perp) \vee (\exists j, k : v_j \neq v_k \wedge v_j, v_k \in \mathcal{R}_p) \\ &\vee (p(\mathbf{x}, \mathbf{y}_c, c) = v_0, v_0 \in \mathcal{R}_p) \wedge (\exists j : v_j \neq v_0, v_j \in \mathcal{R}_p) \end{aligned} \quad (18)$$

The outgoing message $I_{c \rightarrow c'}(\mathbf{y}_s, u)$ is then:

$$I_{c \rightarrow c'}(\mathbf{y}_s, \perp) = \max_{\substack{\mathbf{y}_c \sim \mathbf{y}_s, v_1, \dots, v_l \\ V_2(\mathbf{y}_c, v_1, \dots, v_l)}} \phi_c(\mathbf{y}_c) + \sum_{j=1}^l I_{c_j \rightarrow c}(\mathbf{y}_{s_j}, v_j) \quad (19)$$

After completing the internal message passing schedule, we can compute the final aggregated message $M(u)$ by sending a message from the last clique (wlog, say c') to a dummy root clique r :

$$M(u) \triangleq I_{c' \rightarrow r}(-, u) \quad (20)$$

where the separator labeling is irrelevant because the message is to a dummy clique r .

If $|K| = 1$, then the message $m_{i \rightarrow p}(v)$ is simply $M(v)$. This treatment generalizes nicely to the case when $|K| > 1$. We extend the internal message vector $I(\cdot)$ for each combination of values of the $|K|$ properties. Call it $I_{c \rightarrow c'}(\mathbf{y}_s, u_1, \dots, u_{|K|})$ where $u_j \in \mathcal{R}'_{p_j}$. Let the final aggregated message at a dummy root clique inside instance i be $M(u_1, \dots, u_{|K|})$. The outgoing message $m_{i \rightarrow p}(v)$ to property p can now be computed as:

$$m_{i \rightarrow p}(v) = \max_{\substack{u_1, \dots, u_{|K|} \\ u_p = v}} M(u_1, \dots, u_{|K|}) + \sum_{p' \neq p} m_{p' \rightarrow i}(u_{p'}) \quad (21)$$

The overhead for $|K| > 1$ is that we have to absorb the incoming messages from the other $|K| - 1$ properties, shown in Figure 3 in the red portion.

5.1.2 Approximations

Various approximations are possible to reduce the number of value combinations for which messages have to be maintained.

Typically, the within-instance dependencies are stronger than the dependencies across instances. We can exploit this to reduce the number of property values as follows: First, find the MAP of each instance independently. Only those property values that are fired in the MAP labeling of at least one of the instances are considered in the range. In the application we study in Section 7.2, this reduced the size of the range of properties drastically.

A second trick can be used when properties are associated with labels that tend not to repeat in the MRF, e.g. Title for the citation extraction task. In that case, the value \perp can be ignored. And, we can relax the consistency checks on properties p' that are being absorbed so that they can be absorbed locally at each clique as follows. First, normalize incoming messages from p' as $m_{p' \rightarrow i}(v) - m_{p' \rightarrow i}(\emptyset)$. Next, absorb the normalized message in the clique potential $\phi_c(\mathbf{y}_c)$ of all cliques where $p'(\mathbf{x}, \mathbf{y}_c, c) = v$. Finally, compute the outgoing message by only keeping state over the values of the outgoing property. When the MAP does not contain any repeat firings of a property, this method returns the exact answer.

A third option is to depend on generic search optimization tricks like beam search and rank aggregation. In beam search instead of maintaining messages for each possible combination of property values, we maintain only top-k most promising combinations in each message passing step.

5.2 Message from a Clique to an Instance

The message $m_{p \rightarrow i}(v)$ is computed as:

$$m_{p \rightarrow i}(v) = \max_{\substack{(v_1, \dots, v_n): \\ v_i = v}} \sum_{\substack{j \neq i \\ \mathbf{x}_j \in \mathcal{D}_p}} m_{j \rightarrow p}(v_j) + C_p(\{v_j\}_{\mathbf{x}_j \in \mathcal{D}_p}) \quad (22)$$

Message $m_{p \rightarrow i}(v)$ requires maximizing the objective in Equation 22, which can be re-written as

$$-m_{i \rightarrow p}(v) + \max_{\substack{(v_1, \dots, v_n) \\ v_i = v}} \sum_{j: \mathbf{x}_j \in \mathcal{D}_p} m_{j \rightarrow p}(v_j) + C_p(\{v_j\}_{\mathbf{x}_j \in \mathcal{D}_p})$$

The maximization subtask can be cast in terms of the general *clique inference problem* defined as:

Definition 5.1. *Given a clique over n vertices, with a symmetric clique potential $C(v_1, \dots, v_n)$, and vertex potentials ψ_{jv_j} for all $j \leq n$ and values v_j . Compute the value assignment with the highest potential:*

$$\max_{v_1, \dots, v_n} \sum_{j=1}^n \psi_{jv_j} + C(v_1, \dots, v_n) \quad (23)$$

In our case, $\psi_{jv} \triangleq m_{j \rightarrow p}(v)$ and $C \triangleq C_p$. To compute $m_{p \rightarrow i}(v)$, we can solve the clique inference problem with the restriction $v_i = v$.

We are interested in the cases when the clique potential is Potts or MAJORITY, which were defined in Section 4. These are most popular potentials for real-life collective inference tasks.

In [10], a $\frac{13}{15}$ -approximate clique inference algorithm, called α -pass was presented for C^{Potts} , along with an expensive polynomial-time exact algorithm for C^{Maj} . α -pass can also be applied to arbitrary symmetric potentials and is exact for binary valued properties. The time complexity of α -pass is $O(|\mathcal{R}'_p|n \log n)$, as compared to $(|\mathcal{R}'_p|^2 n^2)$ for ordinary belief propagation.

We next show that although α -pass is also applicable for MAJORITY potentials, it lacks desirable theoretical guarantees. We then present a new approximate inference algorithm for C^{Maj} based on Lagrangian Relaxation which is much faster than the exact algorithm yet produces almost-optimal scores in practice.

6 Algorithms for Clique Inference

In this section we explore various exact and approximate schemes for maximizing the clique inference objective in Definition 5.1 under a variety of symmetric potential functions. Of particular interest are the Potts and MAJORITY potentials, but some of the algorithms are more general and apply to families of potentials.

These clique algorithms are called as subroutines while calculating the messages from property cliques to instances, in accordance with Equation 22. Throughout this section, we assume that the clique corresponds to a fixed property p with range \mathcal{R}'_p . R will be short-hand for $|\mathcal{R}'_p|$.

We will use $F(v_1, \dots, v_n)$ to denote the clique inference objective. As short-hand, we will denote $F(v_1, \dots, v_n)$ by $F(\mathbf{v}) = \psi(\mathbf{v}) + C(\mathbf{v})$ where $\psi(\mathbf{v})$ is the vertex score of \mathbf{v} and the second term is the clique score. Wlog assume that the vertex potentials are positive. Otherwise a constant can be added to all of them and that will not affect the maximization. The best value assignment will be denoted by \mathbf{v}^* , and $\hat{\mathbf{v}}$ will denote an approximate solution.

6.1 α -pass Algorithm

We begin with MAX potentials. These potentials are not used in practice, but clique inference for MAX potentials gives rise to the α -pass algorithm which has very interesting properties. Recall that a MAX potential is of the form $C(\{v_1, \dots, v_n\}) = \max_v f_v(n_v)$. The α -pass algorithm is described in Algorithm 1.

Input: Vertex Potentials ψ , Clique Potential C , set \mathcal{R}'_p of allowed values
Output: Value assignment v_1, \dots, v_n
Best = $-\infty$;
 $\hat{\mathbf{v}} = \text{nil}$;
foreach Value $\alpha \in \mathcal{R}'_p$ **do**
 Sort the vertices by the metric $\psi_{j\alpha} - \max_{v \in \mathcal{R}'_p, v \neq \alpha} \psi_{jv}$;
 foreach $k \in \{1, \dots, n\}$ **do**
 Assign the first k sorted vertices the value α ;
 Assign the remaining vertices their individual best non- α value;
 $s \leftarrow$ score of this assignment;
 if $s > \text{Best}$ **then**
 Best $\leftarrow s$;
 $\hat{\mathbf{v}} \leftarrow$ current assignment;
 end
 end
end
return $\hat{\mathbf{v}}$;

Algorithm 1: The α -pass algorithm

For each (α, k) combination, the α -pass algorithm computes the best k vertices to get the value α . Let $\hat{\mathbf{v}}^{\alpha k}$ denote the complete assignment in the $(\alpha, k)^{\text{th}}$ step. Then it is easy to see that α -pass runs in $O(|\mathcal{R}'_p|n \log n)$ time by incrementally computing $F(\hat{\mathbf{v}}^{\alpha k})$ from $F(\hat{\mathbf{v}}^{\alpha(k-1)})$. We now look at properties of α -pass.

Claim 6.1. *Assignment $\hat{\mathbf{v}}^{\alpha k}$ has the maximum vertex score over all \mathbf{v} where k vertices are assigned α , that is, $\psi(\hat{\mathbf{v}}^{\alpha k}) = \max_{\mathbf{v}: n_\alpha(\mathbf{v})=k} \psi(\mathbf{v})$.*

Proof. This is easily seen by contradiction. If some other assignment $\mathbf{v} \neq \hat{\mathbf{v}}^{\alpha k}$ has the best vertex score, then it differs from $\hat{\mathbf{v}}^{\alpha k}$ in the assignment of at least two vertices, one of which is assigned α in \mathbf{v} and non- α in $\hat{\mathbf{v}}^{\alpha k}$. The converse holds for the other differing vertex. By swapping their assignments, it is possible to increase the vertex score of \mathbf{v} , a contradiction.

Claim 6.2. *For MAX potentials, $C(\hat{\mathbf{v}}^{\alpha k}) \geq f_\alpha(k)$.*

Proof. This is because the value α has a count of k and the MAX potential considers the maximum over all counts.

Theorem 6.1. *The α -pass algorithm finds the MAP for MAX clique potentials.*

Proof. Let \mathbf{v}^* be the optimal assignment and let $\beta = \operatorname{argmax}_v f_v(n_v(\mathbf{v}^*))$, $\ell = n_\beta(\mathbf{v}^*)$. Let $\hat{\mathbf{v}}$ be the assignment

found by α -pass. We have:

$$\begin{aligned}
F(\hat{\mathbf{v}}) &= \max_{1 \leq \alpha \leq |\mathcal{R}'_p|, 1 \leq k \leq n} F(\hat{\mathbf{v}}^{\alpha k}) \\
&\geq F(\hat{\mathbf{v}}^{\beta \ell}) \\
&= \psi(\hat{\mathbf{v}}^{\beta \ell}) + C(\hat{\mathbf{v}}^{\beta \ell}) \\
&\geq \psi(\hat{\mathbf{v}}^{\beta \ell}) + f_\beta(\ell) \\
&= \psi(\hat{\mathbf{v}}^{\beta \ell}) + C(\mathbf{v}^*) \\
&\geq \psi(\mathbf{v}^*) + C(\mathbf{v}^*) \\
&= F(\mathbf{v}^*)
\end{aligned}$$

The second and third inequalities follows from Claims 6.2 and 6.1 respectively. \square

Thus, α -pass finds the optimal assignment for the MAX family of potentials in $O(Rn \log n)$ time. We now move on to SUM potentials.

6.2 Clique Inference for SUM Potentials

We will mainly focus on the Potts potential, which is arguably the most popular member of the SUM family. Potts potential is given by $C(\mathbf{v}) = \lambda \sum_v n_v^2$.

When $\lambda < 0$, the clique edges prefer the two end points to take different values. With negative λ , our objective function $F(\mathbf{v})$ becomes concave and its maximum can be easily found using a relaxed quadratic program followed by an optimal rounding step as suggested in [21]. We therefore do not discuss this case further. The more interesting case is when λ is positive. We show that finding \mathbf{v}^* now becomes NP-hard.

Theorem 6.2. *When $C(\mathbf{v}) = \lambda \sum_v n_v^2$, $\lambda > 0$, finding the MAP assignment is NP-hard.*

Proof. Let $R \triangleq |\mathcal{R}'_p|$. We prove hardness by reducing from the NP-complete *exact cover by 3-sets* problem [19] of deciding if exactly $\frac{2}{3}$ of R subsets S_1, \dots, S_R of 3 elements each from $U = \{e_1, \dots, e_n\}$ can cover U . We let elements correspond to vertices and sets to values. Assign $\psi_{i_v} = 2n\lambda$ if $e_i \in S_v$ and 0 otherwise. MAP score will be $(2n^2 + 3^2 \frac{2}{3})\lambda$ iff we can find an exact cover. \square

The above proof establishes that there cannot be an algorithm that is polynomial in both n and R . But we have not ruled out algorithms with complexity that is polynomial in n but exponential in R , say of the form $O(2^R n^c)$ for a constant c .

We next propose approximation schemes. Unlike for general graphs where the Potts model is approximable only within a factor of $\frac{1}{2}$ [5, 12], we show that for cliques the Potts model can be approximated to within a factor of $\frac{13}{15} \approx 0.86$ using the α -pass algorithm. We first present an easy proof for a weaker bound of $\frac{4}{5}$ and then move on to a more detailed proof for the $\frac{13}{15}$ bound. Recall that the optimal assignment is \mathbf{v}^* and the assignment output by α -pass is $\hat{\mathbf{v}}$.

Theorem 6.3. $F(\hat{\mathbf{v}}) \geq \frac{4}{5}F(\mathbf{v}^*)$.

Proof. Without loss of generality assume that the counts in \mathbf{v}^* are $n_1 \geq n_2 \geq \dots \geq n_R$, where $R = |\mathcal{R}'_p|$. Then $\sum_v n_v^2 \leq n_1 \sum_v n_v = nn_1$.

$$\begin{aligned}
F(\hat{\mathbf{v}}) &\geq F(\hat{\mathbf{v}}^{1n_1}) = \psi(\hat{\mathbf{v}}^{1n_1}) + C(\hat{\mathbf{v}}^{1n_1}) \\
&\geq \psi(\mathbf{v}^*) + C(\hat{\mathbf{v}}^{1n_1}) \quad (\text{from Claim 6.1}) \\
&\geq \psi(\mathbf{v}^*) + \lambda n_1^2 \quad (\text{since } \lambda > 0) \\
&\geq \psi(\mathbf{v}^*) + C(\mathbf{v}^*) - \lambda n_1 n + \lambda n_1^2 \\
&\geq F(\mathbf{v}^*) - \lambda n^2/4
\end{aligned}$$

Now consider the two cases where $F(\mathbf{v}^*) \geq \frac{5}{4}\lambda n^2$ and $F(\mathbf{v}^*) < \frac{5}{4}\lambda n^2$. For the first case we get from above that $F(\hat{\mathbf{v}}) \geq F(\mathbf{v}^*) - \lambda n^2/4 \geq \frac{4}{5}F(\mathbf{v}^*)$. For the second case, we know that the score $F(\hat{\mathbf{v}}^{mn})$ where we assign all vertices the last value is at least λn^2 and thus $F(\hat{\mathbf{v}}) \geq \frac{4}{5}F(\mathbf{v}^*)$. \square

We now state the more involved proof for showing that α -pass actually provides a tighter approximation bound of $\frac{13}{15}$ for Potts potentials.

Theorem 6.4. ¹ $F(\hat{\mathbf{v}}) \geq \frac{13}{15}F(\mathbf{v}^*)$.

Proof. The proof is by contradiction. Suppose there is an instance where $F(\hat{\mathbf{v}}) \leq \frac{13}{15}F(\mathbf{v}^*)$. Wlog assume that $\lambda = 1$ and $n_1 \geq n_2 \geq \dots \geq n_k > 0$, ($2 \leq k \leq R$) be the non-zero counts in the optimal solution and let ψ^* be its vertex potential. Thus $F(\mathbf{v}^*) = \psi^* + n_1^2 + n_2^2 + \dots + n_k^2$.

Now, $F(\hat{\mathbf{v}})$ is at least $\psi^* + n_1^2$ (ref. Claim 6.1). This implies $\frac{\psi^* + n_1^2}{\psi^* + n_1^2 + \dots + n_k^2} \leq \frac{13}{15}$, i.e. $2(\psi^* + n_1^2) < 13(n_2^2 + \dots + n_k^2)$ or

$$\psi^* < \frac{13}{2}(n_2^2 + \dots + n_k^2) - n_1^2 \quad (24)$$

Since k values have non-zero counts, and the vertex score is ψ^* , at least ψ^*/k of the vertex score is assigned to one value. Considering a solution where all vertices are assigned to this value, we get $F(\hat{\mathbf{v}}) \geq \psi^*/k + n^2$.

Therefore $F(\mathbf{v}^*) > 15/13(n^2 + \psi^*/k)$.

Since $F(\mathbf{v}^*) = \psi^* + n_1^2 + \dots + n_k^2$, we get:

$$\psi^* > \frac{15kn^2 - 13k(n_1^2 + \dots + n_k^2)}{13k - 15} \quad (25)$$

We show that Equations 24 and 25 contradict each other. It is sufficient to show that for all $n_1 \geq \dots \geq n_k \geq 1$,

$$\frac{15kn^2 - 13k(n_1^2 + \dots + n_k^2)}{13k - 15} \geq \frac{13}{2}(n_2^2 + \dots + n_k^2) - n_1^2$$

Simplifying, this is equivalent to

$$kn^2 - \frac{13}{2}(k-1)(n_2^2 + \dots + n_k^2) - n_1^2 \geq 0. \quad (26)$$

Consider a sequence n_1, \dots, n_k for which the expression on the left hand side is minimized. If $n_i > n_{i+1}$ then we must have $n_i = 1 \forall i \geq 2$. Otherwise, replace n_{i+1} by $n_{i+1} + 1$ and decrement n_j by 1, where j is the largest index for which $n_j > 1$. This gives a new sequence for which the value of the expression is smaller. Therefore the sequence must be of the form $n_i = n_1$ for $1 \leq i < l$ and $n_i = 1$ for $i > l$, for some $l \geq 2$. Further, considering the expression as a function of n_l , it is quadratic with a negative second derivative. So the minimum occurs at one of the extreme values $n_l = 1$ or $n_l = n_1$. Therefore we only need to consider sequences of the form $n_1, \dots, n_1, 1, \dots, 1$ and show that the expression is non-negative for these.

In such sequences, differentiating with respect to n_1 , the derivative is positive for $n_1 \geq 1$, which means that the expression is minimized for the sequence $1, \dots, 1$. Now it is easy to verify that it is true for such sequences. The expression is zero only for the sequence $1, 1, 1$, which gives the worst case example. \square

The next theorem that the analysis in Theorem 6.4 is tight. We present a pathological example where α -pass gives a solution which is exactly $\frac{13}{15}$ of the optimal.

Theorem 6.5. *The approximation ratio of $\frac{13}{15}$ of the α -pass algorithm is tight.*

Proof. We show an instance where this is obtained. Let $R = n + 3$ and $\lambda = 1$. For the first $n/3$ vertices let $\psi_{u1} = 4n/3$, for the next $n/3$ vertices let $\psi_{u2} = 4n/3$, and for the remaining $n/3$ let $\psi_{u3} = 4n/3$. Also for all vertices let $\psi_{u(u+3)} = 4n/3$. All other vertex potentials are zero. The optimal solution is to assign the first three values $n/3$ vertices each, yielding a score of $4n^2/3 + 3(\frac{n}{3})^2 = 5n^2/3$. The first α -pass on value 1, where initially a vertex u is assigned its vertex optimal value $u + 3$, will assign the first $n/3$ vertices 1. This keeps the sum of total vertex potential unchanged at $4n^2/3$, the clique potential increased to $n^2/9 + 2n/3$ and total score = $4n^2/3 + n^2/9 + 2n/3 = 13n^2/9 + 2n/3$. No subsequent iterations with any other value can improve this score. Thus, the score of α -pass is $\frac{13}{15}$ of the optimal in the limit $n \rightarrow \infty$. \square

¹Thanks to Prof. Diwan for analyzing the α -pass algorithm and its generalization.

6.2.1 α -expansion

In general graphs, a popular method that provides the approximation guarantee of $1/2$ for the Potts model is the graph-cuts based α expansion algorithm [5]. We explore the behavior of this algorithm for Potts potentials.

In this scheme, we start with any initial assignment — for example, all vertices are assigned the first value as suggested in [5]. Next, for each value α we perform an α expansion phase where we switch the assignment of an optimal set of vertices to α from their current value. We repeat this until in a round over the R values, no vertices switch their assignment.

For graphs whose edge potentials form a metric, an optimal α expansion move is based on the use of the mincut algorithm of [5] which for the case of cliques can be $O(n^3)$.

We next show how to perform optimal α expansion moves more efficiently for all kinds of SUM potentials.

An α expansion move Let $\tilde{\mathbf{v}}$ be the assignment at the start of this move. For each value $v \neq \alpha$ create a sorted list S_v of vertices assigned v in $\tilde{\mathbf{v}}$ in decreasing order of $\psi_{i\alpha} - \psi_{iv}$. If in an optimal move, we move k_v vertices from v to α , then it is clear that we need to pick the top k_v vertices from S_v . Let r_i be the rank of a vertex i in S_v . Our remaining task is to decide the optimal number k_v to take from each S_v . We find these using dynamic programming. Without loss of generality assume $\alpha = R$ and $1, \dots, R-1$ are the $R-1$ values other than α .

Let $D_j(k)$ denote the best score with k vertices assigned values from $1 \dots j$ switched to α . We compute

$$D_j(k) = \max_{l \leq k, l \leq n_j(\tilde{\mathbf{v}})} D_{j-1}(k-l) + f_j(n_j(\tilde{\mathbf{v}}) - l) + \sum_{i:r_{i'} \leq l} \psi_{i'\alpha} + \sum_{i:r_{i'} > l} \psi_{i'j}$$

From here we can calculate the optimal number of vertices to switch to α as $\operatorname{argmax}_{k \leq n - n_\alpha(\tilde{\mathbf{v}})} D_{R-1}(k) + f_\alpha(k + n_\alpha(\tilde{\mathbf{v}}))$.

Theorem 6.6. *The α -expansion algorithm provides no better approximation guarantee than $1/2$ even for the special case of homogeneous Potts potential on cliques.*

Proof. Consider an instance where $R = k + 1$, and $\lambda = 1$. Let $\psi_{u1} = 2n/k$ for all u and for k disjoint groups of n/k vertices each, let $\psi_{u,i+1} = 2n$ for the vertices in the i^{th} group. All other vertex potentials are zero. Consider the solution where every vertex is assigned value 1. This assignment is locally optimal wrt any α -expansion move, and its score is $n^2(1 + 2/k)$. However, the exact solution assigns every vertex group its value, with a score $n^2(2 + 1/k)$, thus giving a ratio of $1/2$ in the limit. \square

We next present a generalization of the α -pass algorithm that provides provably better guarantees while being faster than α -expansion.

6.2.2 Generalized α -pass algorithm

In α -pass for each value α , we go over each count k and find the best vertex score with k vertices assigned value α . We generalize this to go over all value combinations of size no more than q , a parameter of the algorithm that is fixed based on the desired approximation guarantee.

For each value subset $A \subseteq \mathcal{R}'_p$ of size no more than q , and for each count k , maximize vertex potentials with k vertices assigned a value from set A . For this, sort vertices in decreasing order of $\max_{\alpha \in A} \psi_{i\alpha} - \max_{v \notin A} \psi_{iv}$, assign the top k vertices their best value in A and the remaining their best value not in A . The best solution over all A, k with $|A| \leq q$ is the final assignment $\hat{\mathbf{v}}$.

The complexity of this algorithm is $O(nR^q \log n)$. In practice, we can use heuristics to prune the number of value combinations. Further, we can make the following claims about the quality of its output.

Theorem 6.7. $F(\hat{\mathbf{v}}) \geq \frac{8}{9}F(\mathbf{v}^*)$.

Proof. This bound is achieved if we run the algorithm with $q = 2$. Let the optimal solution have counts $n_1 \geq n_2 \geq \dots \geq n_R$ and let its vertex potential be ψ^* . For simplicity let $a = n_1/n$, $b = n_2/n$ and $c = \psi^*/n^2$. Then $F(\mathbf{v}^*)/n^2 \leq c + a^2 + b(1-a)$, $F(\hat{\mathbf{v}})/n^2 \geq c + a^2$ and $F(\hat{\mathbf{v}})/n^2 \geq c + \frac{(a+b)^2}{2}$.

Case 1: $a^2 \geq \frac{(a+b)^2}{2}$. Then $F(\mathbf{v}^*) - F(\hat{\mathbf{v}}) \leq bn^2(1-a)$. For a given value of a , this is maximized when b is as large as possible. For Case 1 to hold, the largest possible value of b is given by $a^2 = \frac{(a+b)^2}{2}$, which gives $b = a(\sqrt{2} - 1)$. Therefore $F(\mathbf{v}^*) - F(\hat{\mathbf{v}}) \leq \frac{n^2(\sqrt{2}-1)}{4} < \frac{n^2}{8}$, i.e. $F(\hat{\mathbf{v}}) \geq \frac{8}{9}F(\mathbf{v}^*)$.

Case 2: $a^2 \leq \frac{(a+b)^2}{2}$. This holds if $b \geq (\sqrt{2} - 1)a$. Since $a + b \leq 1$, this is possible only if $a \leq 1/\sqrt{2}$. Now $\frac{F(\mathbf{v}^*) - F(\hat{\mathbf{v}})}{n^2} \leq a^2 + b(1-a) - (a+b)^2/2 = \frac{a^2 - 4ab + 2b - b^2}{2}$.

For a given a , this expression is quadratic in b with a negative second derivative. This is maximized (by differentiating) for $b = 1 - 2a$. Since $b \leq a$, this value is possible only if $a \geq 1/3$. Similarly, for case 2 to hold with this value of b , we must have $a \leq \sqrt{2} - 1$. Substituting this value of b , the difference in scores is $\frac{5a^2 - 4a + 1}{2}$.

Since this is quadratic with a positive second derivative, it is maximized when a has either the minimum or maximum possible value. For $a = 1/3$ this value is $1/9$, while for $a = \sqrt{2} - 1$, it is $10 - 7\sqrt{2}$. In both cases, it is less than $1/8$.

If $a \leq 1/3$ the maximum is achieved when $b = a$. In this case, the score difference is at most $(a - 2a^2)$ which is maximized for $a = 1/4$, where the value is $1/8$. (This is the worst case).

For $\sqrt{2} - 1 < a \leq 1/\sqrt{2}$, the maximum will occur for $b = (\sqrt{2} - 1)a$. Substituting this value for b , the score difference is $(\sqrt{2} - 1)(a - a^2)$, which is maximized for $a = 1/2$, where its value is $(\sqrt{2} - 1)/4 < 1/8$. \square

We believe that the bound for general q is $\frac{4q}{4q+1}$. This bound is not tight as for $q = 1$ we have already shown that the $\frac{4}{5}$ bound can be tightened to $\frac{13}{15}$. With $q = 2$ we get a bound of $\frac{8}{9}$ which is better than $\frac{13}{15}$.

Entropy potentials and the α -pass algorithm

As an aside, let us explore the behavior of α -pass on another family of additive potentials — entropy potentials. Entropy potentials are of the form:

$$C(\mathbf{v}) = \lambda \sum_v n_v \log n_v, \text{ where } \lambda > 0 \quad (27)$$

The main reason α -pass provides a good bound for Potts potentials is that it guarantees a clique potential of at least n_1^2 where n_1 is the count of the most dominant value in the optimal solution. The quadratic term compensates for possible sub-optimality of counts of other values. If we had a sub-quadratic term instead, say $n_1 \log n_1$ for the entropy potentials, the same bound would not have held. In fact the following theorem shows that for entropy potentials, even though α -pass guarantees a clique potential of at least $n_1 \log n_1$, that is not enough to provide a good approximation ratio.

Theorem 6.8. *α -pass does not provide a bound better than $\frac{1}{2}$ for entropy potentials.*

Proof. Consider a counter example where there are $R = n + \log n$ values. Divide the values into two sets — A with $\log n$ values and B with n values. The vertex potentials are as follows: the vertices are divided into $\log n$ chunks of size $n/\log n$ each. If the j^{th} vertex lies in the v^{th} chunk, then let it have a vertex potential of $\log n$ with value v in A and a vertex potential of $\log n + \epsilon$ with the j^{th} vertex in B . Let all other vertex potentials be zero. Also, let $\lambda = 1$.

Consider the assignment which assigns the v^{th} value in A to the v^{th} chunk. Its score is $2n \log n - n \log \log n$. Now consider α -pass, with $\alpha \in A$. Initially vertex v will be set to the v^{th} value in B . The best assignment found by α -pass will assign every vertex to α , for a total score of roughly $n + n \log n$. If $\alpha \in B$, then again the best assignment will assign everything to α for a total score of roughly $(n + 1) \log n$.

Thus the bound is no better than $\frac{1}{2}$ as $n \rightarrow \infty$. \square

Thus, α -pass provides good approximations when the clique potential is dominated by the most dominated value. We now look at MAJORITY potentials, which are linear in the counts $\{n_v\}_v$. Looking at Theorem 6.8, we expect that α -pass will not have decent approximation guarantees for MAJORITY. This is indeed the case. We will prove in Section 6.3 that neither α -pass nor a natural modification of α -pass enjoy good approximation guarantees.

6.3 Clique Inference for MAJORITY Potentials

Recall that MAJORITY potentials are of the form $C = f_a(\mathbf{n})$, $a = \operatorname{argmax}_v n_v$. We consider linear majority potentials where $f_a(\mathbf{n}) = \sum_v w_{av} n_v$. The matrix $W = \{w_{vv'}\}$ is not necessarily diagonally dominant or symmetric.

We show that exact MAP for linear majority potentials can be found in polynomial time. We also present a modification to the α -pass algorithm to serve as an efficient heuristic, but without approximation guarantees. Then we present a Lagrangian relaxation based approximation, whose runtime in practice is similar to α -pass, but provides much better solutions.

6.3.1 Modified α -pass algorithm

In the case of linear majority potentials, we can incorporate the clique term in the vertex potential, and this leads to the following modifications to the α -pass algorithm: (a) Sort the list for α according to the modified metric $\psi_{i\alpha} + w_{\alpha\alpha} - \max_{v \neq \alpha} (\psi_{iv} + w_{\alpha v})$, and (b) While sweeping the list for α , discard all candidate solutions whose majority value is not α .

However even after these modifications, α -pass does not provide the same approximate guarantee as for homogeneous Potts potentials, as we prove next. We denote a matrix W as diagonally dominant iff each of its diagonal entries are the largest in their corresponding rows.

Theorem 6.9. *The modified α -pass algorithm cannot have an approximation ratio better than $\frac{1}{2}$ on linear majority potentials with unconstrained W .*

Proof. Consider the degenerate example where all vertex potentials are zero. Let β and γ be two fixed values and let the matrix W be defined as follows: $w_{\beta\gamma} = M + \epsilon$, $w_{\beta v} = M \forall v \neq \beta, \gamma$ and all the other entries in W are zero.

In modified α -pass, when $\alpha \neq \beta$, the assignment returned will have a zero score. When $\alpha = \beta$, all vertices will prefer the value γ , so α -pass will have to assign exactly $n/2$ vertices as β to make it the majority value, thus returning a score of $\frac{(M+\epsilon)n}{2}$. However, consider the assignment which assigns n/R vertices to each value, with a score of $(R-1)Mn/R$. Hence the approximation ratio cannot be better than $\frac{1}{2}$. \square

Theorem 6.10. *The modified α -pass algorithm cannot provide an approximation bound better than $\frac{2}{3}$ for linear MAJORITY potentials even when W is diagonally dominant and each of its rows have equal sums.*

Proof. The proof is by counter example which is constructed as follows. Let the set of values \mathcal{R}'_p be divided into two subsets, A and B with k and $n-k$ values respectively, where $k < n/2$. Let $\beta \in B$ be a fixed value. We define W as:

$$w_{vv'} = \begin{cases} n-k & v, v' \in A \\ k+1 & v \in A, v' = \beta \\ k+1 & v, v' \in B \\ 0 & \text{otherwise} \end{cases}$$

Thus W is diagonally dominant with all rows summing to $(n-k)(k+1)$.

The vertex potentials ψ are defined as follows. Divide the vertices into k chunks of size n/k each. For the v^{th} value in A , each vertex in the v^{th} chunk has a vertex potential of $2(n-k)$. Further, $\psi_{i\beta} = 2(n-k) \forall i$. The remaining vertex potentials are zero.

The optimal solution is obtained by assigning the v^{th} value in A to the v^{th} chunk, with a total score of $\frac{n}{k} \cdot 2(n-k) \cdot k + (n-k) \cdot \frac{n}{k} \cdot k = 3n(n-k)$.

In α -pass, consider the pass for $\alpha \in A$. Each vertex i prefers β because $\psi_{i\beta} + w_{\alpha\beta} = 3(n-k)$ is the best across all values. Thus, the best α -pass generated assignment with majority value α is one where we assign $n/2$ vertices α , including the n/k vertices that correspond to the chunk of α . The vertex and clique potentials of this assignment are $\frac{n}{k} \cdot 2(n-k) + \frac{n}{2} \cdot 2(n-k)$ and $\frac{n}{2}(n-k) + \frac{n}{2}(n-k)$, giving a total score of $2n(n-k) + \frac{2n(n-k)}{k}$. This gives an approximation ratio of $\frac{2}{3}(1 + \frac{1}{k})$.

Now consider the pass when $\alpha \in B$. Each vertex i again prefers β because $\psi_{i\beta} + w_{\alpha\beta} = 2n-k+1$ is the best across all values. If $\alpha = \beta$, the best α -pass assignment is one where all vertices are assigned β , giving a total

cost of $n(2n - k + 1)$. If $\alpha \neq \beta$, then to make α the majority value, α -pass can only output an assignment with score less than $n(2n - k + 1)$. In this case, the approximation ratio is no better than $\frac{2n-k+1}{3(n-k)}$.

Setting $k = \sqrt{n}$ and $n \rightarrow \infty$, we get the desired result. \square

However, in practice where the W matrix is typically sparse, our experiments in Section 7.1 show that α -pass performs well and is significantly more efficient than the exact algorithm described next.

6.3.2 Exact Algorithm

Since MAJORITY potentials are linear, we can pose the optimization problem in terms of Integer Programs (IPs). Assume that we know the majority value α . Then, the optimization problem corresponds to the IP:

$$\begin{aligned} \max_{\mathbf{z}} \quad & \sum_{i,v} (\psi_{iv} + w_{\alpha v}) z_{iv} \\ \forall v : \quad & \sum_i z_{iv} \leq \sum_i z_{i\alpha}, \\ \forall i : \quad & \sum_v z_{iv} = 1, \quad z_{iv} \in \{0, 1\} \end{aligned} \tag{28}$$

We can solve R such IPs by guessing various values as the majority value, and reporting the best overall assignment as the output. However, Equation 28 cannot be relaxed to a linear program. This can be easily shown by proving that the constraint matrix is not totally unimodular. Alternatively, here is a counter example: Consider a 3-node, 3-value graphical model with a zero W matrix. Let the vertex potential vectors be $\psi_0 = (1, 4, 0)$, $\psi_1 = (4, 0, 4)$, $\psi_2 = (3, 4, 0)$. While solving for $\alpha = 0$, the best IP assignment is 1, 0, 0 with a score of 11. However the LP relaxation has the solution $\mathbf{z} = (0, 1, 0; 1, 0, 0; 1/2, 1/2, 0)$ with a score of 11.5.

This issue can be resolved by making the constraint matrix totally unimodular as follows. Guess the majority value α , the count $k = n_\alpha$, and solve the following IP:

$$\begin{aligned} \max_{\mathbf{z}} \quad & \sum_{i,v} (\psi_{iv} + w_{\alpha v}) z_{iv} \\ \forall v \neq \alpha : \quad & \sum_i z_{iv} \leq k, \\ & \sum_i z_{i\alpha} = k, \\ \forall i : \quad & \sum_v z_{iv} = 1, \quad z_{iv} \in \{0, 1\} \end{aligned} \tag{29}$$

This IP solves the degree constrained bipartite matching problem, which can be solved exactly in polynomial time. Indeed, it can be shown that the LP relaxation of this IP has an integral solution.

Theorem 6.11. *The integer program in Equation 29 has a tight LP relaxation.*

Proof. Denote the constraint matrix of program 29 by $A_{(m+n) \times mn}$, and let A_1 and A_2 denote its first $m - 1$ and last $n + 1$ rows respectively. The $n + 1$ equality constraints can be converted into ' \leq ' constraints by adding negative slack variables. For example, $s_i + \sum_v z_{iv} \leq 1$ and $s_\alpha + \sum_i z_{i\alpha} \leq k$. The variables are now $(\mathbf{z}, \mathbf{s})^T$, and the extra constraints are $\mathbf{s} \leq \mathbf{0}$. The new constraint matrix of this system (which has only inequality constraints)

is given by $B = \begin{bmatrix} A_1 & 0 \\ A_2 & I \\ 0 & I \end{bmatrix}$. The tightness of the LP relaxation follows if B is totally unimodular. For that, it

suffices to prove that $A = \begin{bmatrix} A_1 \\ A_2 \end{bmatrix}$ is totally unimodular. This is so because then $\begin{bmatrix} A_1 & 0 \\ A_2 & I \end{bmatrix}$ would be totally unimodular, and by extension of the same argument, so would be B . The total unimodularity of A is proven as follows.

Let C be an arbitrary $t \times t$ sub-matrix of A . Our argument uses induction on t , with the base case $t = 1$ being straightforward. Note that each column in A has exactly two 1's. Let B_1 denote the first m rows and B_2 denote the remaining n rows of A .

Case 1: C has a column with all zeros. Then $\det(C) = 0$ and we are done.

Case 2: C lies totally inside either B_1 or B_2 . Since there is only one non-zero entry in each column of B_1 (or B_2), pick any column and $\det(C)$ will be ± 1 times the determinant of its $(t-1) \times (t-1)$ sub-matrix, depending on the column index. So using the induction hypothesis, we get $\det(C) \in \{0, \pm 1\}$.

Case 3: C spans rows in B_1 and B_2 . Wlog assume that each column in C has exactly two 1's, otherwise we can apply the same argument as Case 1 or 2. Now, summing up the rows corresponding to B_1 and B_2 separately, we get $\forall j : \sum_{i \in \text{rows}(B_1)} c_{ij} = 1 = \sum_{i \in \text{rows}(B_2)} c_{ij}$. Hence the rows of C are linearly dependent and so $\det(C) = 0$. \square

Thus we can solve $O(Rn)$ such problems by varying α and k , and report the best solution. We believe that since the subproblems are related, it should be possible to solve them incrementally using combinatorial approaches.

6.3.3 Lagrangian Relaxation based Algorithm for MAJORITY Potentials

Solving the linear system in Equation 29 is very expensive because we need to solve $O(Rn)$ LPs, whereas the system in Equation 28 cannot be solved exactly using a linear relaxation. Here, we look at a Lagrangian Relaxation based approach, where we solve the system in Equation 28 but bypass the troublesome constraint $\forall v \neq \alpha : \sum_i z_{iv} \leq \sum_i z_{i\alpha}$.

We make use of the Lagrangian Relaxation technique to move the troublesome majority constraint to the objective function. Any violation of this constraint is penalized by a positive penalty term. Consider the following modified program, also called the Lagrangian:

$$L(\gamma) = L(\gamma_1, \dots, \gamma_R) = \max_{\mathbf{z}} \sum_{i,v} (\psi_{iv} + w_{\alpha v}) z_{iv} + \sum_v \gamma_v (\sum_i z_{i\alpha} - \sum_i z_{iv})$$

$$\forall i : \sum_v z_{iv} = 1 \quad , \quad z_{iv} \in \{0, 1\} \quad (30)$$

For $\gamma \geq \mathbf{0}$, and feasible assignments \mathbf{z} , $L(\gamma)$ is an upper bound for our objective in Equation 28. Thus, we compute the lowest such upper bound:

$$L^* = \min_{\gamma \geq \mathbf{0}} L(\gamma) \quad (31)$$

Since the penalty term in Equation 30 is linear in \mathbf{z} , we can merge it with the first term to get another set of modified vertex potentials:

$$\psi_{iv}^\alpha \triangleq \psi_{iv} + w_{\alpha v} - \gamma_v + \begin{cases} \sum_{v'} \gamma_{v'} & v = \alpha \\ 0 & v \neq \alpha \end{cases} \quad (32)$$

Equation 30 can now be rewritten in terms of ψ^α , with the only constraint that \mathbf{z} be a assignment:

$$\max_{\mathbf{z}} \sum_{i,v} \psi_{iv}^\alpha z_{iv}$$

$$\forall i : \sum_v z_{iv} = 1, \quad z_{iv} \in \{0, 1\} \quad (33)$$

Hence, $L(\gamma)$ can be computed by independently assigning each vertex i to its best value, viz. $\arg \max_v \psi_{iv}^\alpha$.

We now focus on computing L^* . We use an iterative approach, beginning with $\gamma = \mathbf{0}$, and carefully choose a new γ at each step to get a non-increasing sequence of $L(\gamma)$'s. We describe the method of choosing a new γ later in this section, and instead outline sufficient conditions for termination and detection of optimality.

Theorem 6.12. \mathbf{z}^* and γ^* are optimum solutions to Equations 28 and 31 respectively if they satisfy the conditions:

$$\forall v : \sum_i z_{iv}^* \leq \sum_i z_{i\alpha}^* \quad (34)$$

$$\forall v : |\gamma_y^* (\sum_i z_{iv}^* - \sum_i z_{i\alpha}^*)| = 0 \quad (35)$$

Theorem 6.12 holds only for fractional \mathbf{z}^* . To see how, consider an example with 3 vertices and 2 values. Let $\psi_{i0} + w_{\alpha 0} > \psi_{i1} + w_{\alpha 1}$ for all i and α . During Lagrangian relaxation with $\alpha = 1$, initially $\gamma = \mathbf{0}$ will cause all vertices to be assigned value 0, violating Equation 34. Since the count difference $\sum_i z_{i0} - \sum_i z_{i1} \in \{\pm 1, \pm 2, \pm 3\}$, any non-zero γ_0 will violate Equation 35. Subsequent reduction of γ_0 to zero will again cause the original violation of Equation 34. Consequently, one of Equations 34 and 35 will never be satisfied and the algorithm will oscillate.

To tackle this, we relax Equation 35 to $|\gamma_v (\sum_i z_{iv}^* - \sum_i z_{i\alpha}^*)| \leq \epsilon$, where ϵ is a small fraction of an upper bound on γ_v , whose computation is illustrated later. This helps in reporting assignments that respect the majority constraint in Equation 34 and are close to the optimal.

The outline of the algorithm is described in Figure 2. We now discuss a few possible approaches to select a new γ at every step.

Subgradient Optimization

This approach can be used to change all components of γ in a single step. Subgradient optimization generates a sequence of direction vectors $\{\mathbf{d}^1, \mathbf{d}^2, \dots\}$ and positive step sizes $\{\eta_1, \eta_2, \dots\}$. At the k^{th} step, the γ vector is changed as:

$$\gamma_v \leftarrow \max(0, \gamma_v + \eta_k \mathbf{d}^k) \quad (36)$$

In its simplest form, the direction \mathbf{d}^k is the violation vector $(\sum_i z_{iv} - \sum_i z_{i\alpha})_{v=1\dots R}$. Thus, if a value v has a count greater than α , then γ_v will be increased to take some vertices away from v . In practice though, \mathbf{d}^k is usually a convex combination of the violation vector and the previous direction \mathbf{d}^{k-1} . This helps in avoiding oscillations of the kind where γ^{k+2} is very close to γ^k , while simultaneously moving closer to the optimum.

The subgradient optimization framework allows various ways to choose the step sizes. For example, if we choose to set the direction using only the violation vector, then a sequence $\{\eta_1, \eta_2, \dots\}$ of step sizes satisfying (i) $\lim_{k \rightarrow \infty} \eta_k = 0$ and (ii) $\sum_{k=0}^{\infty} \eta_k = \infty$ will ensure asymptotic convergence [11]. These are not the only set of sufficient conditions that guarantee convergence. Practical implementations often compute η_k using the current value of $L(\gamma)$, current violations, and a few user defined parameters.

However, during experimentation the degrees of freedom in choosing the step sizes posed a big problem for us. Since a single step size is shared across all components of γ , a large step size moved everything to α , while a small step size considerably slowed down convergence. Data independent approaches to choosing step sizes also failed to converge in a reasonable number of iterations. In general, subgradient optimization is known to require very careful tweaking of the step sizes across iterations in order to achieve meaningful convergence speeds [11]. For this reason, we looked at alternate approaches to change γ .

Golden Search based Coordinate Descent

If all components of γ except one (say γ_v), are kept fixed, then $L(\gamma)$ is a quasi-convex function of γ_v . Thus, it has a unique global minima, which can be found using golden search, which is an efficient line search method. We choose the value v , whose corresponding violation is the highest in magnitude.

Golden search requires lower and upper bounds on γ_v and evaluates $L(\gamma)$ at various γ 's inside that interval. As before, $L(\gamma)$ can be easily obtained by a computing an assignment which is vertex-optimal wrt the ψ^α 's. We use the trivial lower bound of zero, and estimate a good upper bound from the current solution state. If currently $\sum_i z_{iv} \leq \sum_u z_{u\alpha}$, then γ_v (which is a penalty parameter) can be decreased, and therefore the current value of γ_v can serve as an upper bound. On the other hand, if we start increasing γ_v , then one by one, the vertices currently assigned v will switch to their next best values, and by a particular increased value of γ_v , all vertices assigned v would have flipped. There is no need to increase γ_v beyond this point, so we use this value of γ_v as our upper bound, which can thus be summarized as :

$$UB(v) = \max_{i: z_{iv}=1} \delta_i$$

where (denoting the current second best value of i by β),

$$\delta_i = \begin{cases} \psi_{iv} + w_{\alpha v} - \psi_{i\beta} - w_{\alpha\beta} + \gamma_\beta & \beta \neq \alpha \\ \frac{1}{2}(\psi_{iv} + w_{\alpha v} - \psi_{i\alpha} - w_{\alpha\alpha} - \sum_{\beta \neq v} \gamma_\beta) & \beta = \alpha \end{cases}$$

In spite of its simplicity, Golden Search suffers from a few drawbacks that come to light during experimentation. First, it always performs $\theta(\log UB(v))$ evaluations of $L(\gamma)$. This can drive up the overall runtime of the algorithm. Second, a change in γ_v affects the modified vertex potentials for values v and α (Equation 32). Thus, a large change in γ_v may flip many vertices to α , causing a big change in the current assignment \mathbf{z} , and we may end up spending the next few iterations repairing these changes. Third, line search methods zero-in on the optima by evaluating the objective at various points and choosing a sub-interval accordingly. In our case, due to the integrality of \mathbf{z} , ties can happen at many places in an interval. In such a scenario, arbitrary tie resolution may cause a wrong sub-interval to be chosen for further consideration.

To tackle these issues, we use a more conservative coordinate descent approach, which we describe next and also use in our experiments.

Conservative Coordinate Descent

We can avoid a large number of flips in the current assignment if we replace our golden search method with a more conservative one. Let v be the worst violating value in the current iteration. We will first consider the case when its count exceeds that of α , so that Equation 34 does not hold.

To decrease the count of v , we need to increase γ_v . Let i be a vertex currently assigned v and let $\beta(i)$ be its second most preferred value under the vertex potentials ψ_i^α . The vertex $j = \operatorname{argmax}_{i:z_{iv}=1} \psi_{i\beta(i)}^\alpha - \psi_{iv}^\alpha$ is the easiest to flip. So we increase γ_v till the point when this difference becomes zero. The new value of γ_v is therefore given by:

$$\gamma_v = \min_{i:z_{iv}=1} \begin{cases} \Delta\psi(i, v, \beta(i)) + \gamma_{\beta(i)} & \beta(i) \neq \alpha \\ \frac{1}{2}(\Delta\psi(i, v, \alpha) - \sum_{v' \neq v} \gamma_{v'}) & \beta(i) = \alpha \end{cases} \quad (37)$$

where $\Delta\psi(i, v, v')$ denotes $\psi_{iv} + w_{\alpha v} - \psi_{iv'} - w_{\alpha v'}$. It is possible that by flipping vertex j , $\beta(j)$ now violates Equation 34. Further, increasing γ_v also increases $\psi_{i\alpha}^\alpha$, so some other vertices that are not assigned v may also move to α . However since the change is conservative, we expect this behavior to be limited. In our experiments, we found that this conservative scheme converges much faster than golden section over a variety of data.

We now look at the case when Equation 34 is satisfied by all values but Equation 35 is violated by some value v . In this scenario, we need to decrease γ_v to decrease the magnitude of the violation. Here too, we conservatively decrease γ_v barely enough to flip one vertex to v . If i is any vertex not assigned value v and $\beta(i)$ is its current value, then the new value of γ_v is given by:

$$\gamma_v = \max_{i:z_{iv} \neq 1} \begin{cases} \Delta\psi(i, v, \beta(i)) + \gamma_{\beta(i)} & \beta(i) \neq \alpha \\ \frac{1}{2}(\Delta\psi(i, v, \alpha) - \sum_{v' \neq v} \gamma_{v'}) & \beta(i) = \alpha \end{cases} \quad (38)$$

Note that the arguments of Equations 37 and 38 are the same. In this case too, in spite of a conservative move, more than one vertex marked α may flip to some other value, although at most one of them will be flipped to v . As before, the small magnitude of the change restricts this behavior in practice.

7 Applications and Experiments

We present results of three different experiments.

First, in Section 7.1 we compare our clique inference algorithms against applicable alternatives in the literature. We compare the algorithms on speed and accuracy of the output assignments. For Potts potentials, we show that α -pass is superior to the TRW-S and min-cut based algorithms. For MAJORITY potentials, we compare the modified α -pass and Lagrangian relaxation based algorithms against the exact LP-based approach and the iterated conditional modes (ICM) algorithm.

Input: $\psi, W, \alpha, \text{maxIters}, \text{tolerance}$
Output: approximately best assignment $\hat{\mathbf{v}}$
 $\gamma \leftarrow \mathbf{0}$;
 $\text{iter} \leftarrow 0$;
 $\hat{\mathbf{z}} \leftarrow$ Assignment with all vertices assigned α ;
while $\text{iter} < \text{maxIters}$ **do**
 Compute $L(\gamma)$ (Equation 30), let \mathbf{z} be the solution;
 if $F(\mathbf{z}) > F(\hat{\mathbf{z}})$ **then**
 $\hat{\mathbf{z}} \leftarrow \mathbf{z}$;
 end
 $(v, \Delta) \leftarrow$ Worst violator and violation (Equations 34 and 35);
 if $\Delta < \text{tolerance}$ **then**
 We are done, $L^* = L(\gamma)$;
 break *break*;
 else if *using subgradient optimization* **then**
 Compute the new direction \mathbf{d}^{iter} and step-size η^{iter} ;
 Modify γ using Equation 36;
 else
 Modify γ_v using golden search or conservative descent;
 end
 $\text{iter} \leftarrow \text{iter} + 1$;
end
Construct value assignment $\hat{\mathbf{v}}$ from $\hat{\mathbf{z}}$;
return $\hat{\mathbf{v}}$

Algorithm 2: Compute L^*

Second, in Section 7.2 we demonstrate the application of the generalized collective framework on domain adaptation and show that using a good set of properties can bring down the test error significantly. Finally, in Section 7.3 we show that message passing on the cluster graph is a more effective way to perform inference compared to alternatives such as ordinary belief propagation, and enjoys better convergence speeds.

7.1 Clique Inference Experiments

In this section, we compare our algorithms against sequential tree re-weighted message passing (TRW-S) and graph-cut based inference for clique potentials that are decomposable over clique edges; and with ICM when the clique potentials are not edge decomposable. We compare them on running time and quality of the MAP. Our experiments were performed on both synthetic and real data.

Synthetic Dataset: We generated cliques with 100 vertices and $R = 24$ values by choosing vertex potentials at random from $[0, 2]$ for all values. A Potts version (POTTS) was created by gradually varying λ , and generating 25 cliques for every value of λ . We also created analogous ENTROPY, MAKESPAN and MAKESPAN2 versions of the dataset by choosing entropy, linear makespan ($\lambda \max_v n_v$) and square makespan ($\lambda \max_v n_v^2$) clique potentials respectively.

For MAJORITY potentials we generated two kinds of datasets (parameterized by λ): (a) MAJ-DENSE obtained by generating a random symmetric W for each clique, where $W_{vv} = \lambda$ was the same for all v and $W_{vv'} \in [0, 2\lambda]$ ($v \neq v'$), and (b) MAJ-SPARSE from symmetric W with $W_{ij} \in [0, 2\lambda]$ for all i, j , roughly 70% of whose entries were zeroed.

Of these, only POTTS is decomposable over clique edges.

CoNLL Dataset: The CoNLL 2003 dataset² is a popular choice for demonstrating the benefit of collective labeling in named entity recognition tasks. We used the BIOES encoding of the entities, that resulted in 20 labels. We took a subset of 1460 records from the test set of CoNLL, and selected all 233 cliques of size 10 and above. The median and largest clique sizes were 16 and 259 respectively. The vertex potentials of the cliques were set by a sequential Conditional Random Field trained on a separate training set. We created a Potts version by

²<http://cnts.uia.ac.be/conll2003/ner/>

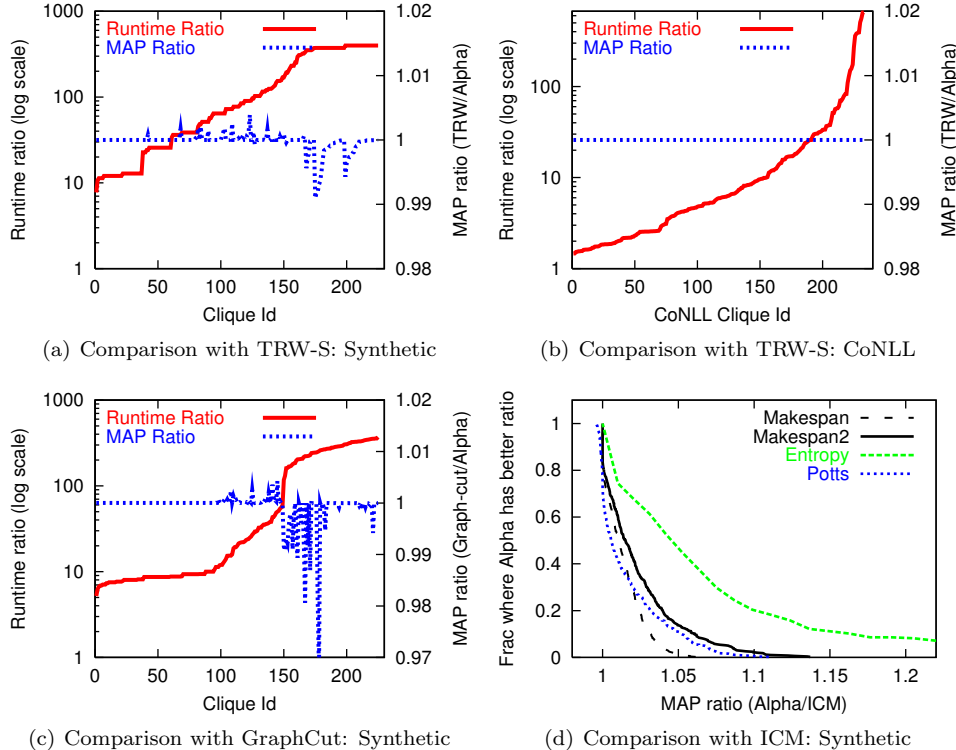


Figure 4: Comparison with TRW-S, Graph-cut and ICM

setting $\lambda = 0.9/n$, where n is the clique size. Such a λ allowed us to balance the vertex and clique potentials for each clique. A majority version was also created by learning W discriminatively in the training phase.

All our algorithms were written in Java. We compared these with C++ implementations of the TRW-S³, and graph-cut based expansion algorithms⁴ [5, 23, 14, 4]. All experiments were performed on a Pentium-IV 3.0 GHz machine with four processors and 2 GB of RAM.

7.1.1 Edge decomposable potentials

Figures 4(a) and 4(b) compare the performance of TRW-S vs α -pass on the two datasets. In Figure 4(a), we varied λ uniformly in $[0.8, 1.2]$ with increments of 0.05. This range of λ is of special interest, because it allows maximal contention between the clique and vertex potentials. For λ outside this range, the MAP is almost always a trivial assignment, viz. one which individually assigns each vertex to its best value, or assigns all vertices to a single value.

We compare two metrics — (a) the quality of the MAP score, captured by the ratio of the TRW-S MAP score with the α -pass MAP score, and (b) the runtime required to report that MAP, again as a ratio. Figure 4(a) shows that while both the approaches report almost similar MAP scores, the TRW-S algorithm is more than 10 times slower in more than 80% of the cases, and is never faster. This is expected because each iteration of TRW-S costs $O(n^2)$, and multiple iterations must be undertaken. In terms of absolute run times, a single iteration of TRW-S took an average of 193ms across all cliques in POTS, whereas our algorithm returned the MAP in 27.6 ± 8.7 ms. Similar behavior can be observed on CoNLL dataset in Figure 4(b). Though the degradation is not as much as before, mainly because of the smaller average clique size, TRW-S is more than 5 times slower on more than half the cliques.

Figure 4(c) shows the comparison with Graph-cut based expansion. The MAP ratio is even more in favor of α -pass, while the blowup in running time is of the same order of magnitude as TRW-S. This is surprising

³<http://www.adastral.ucl.ac.uk/~vladkolm/papers/TRW-S.html>

⁴<http://vision.middlebury.edu/MRF/>

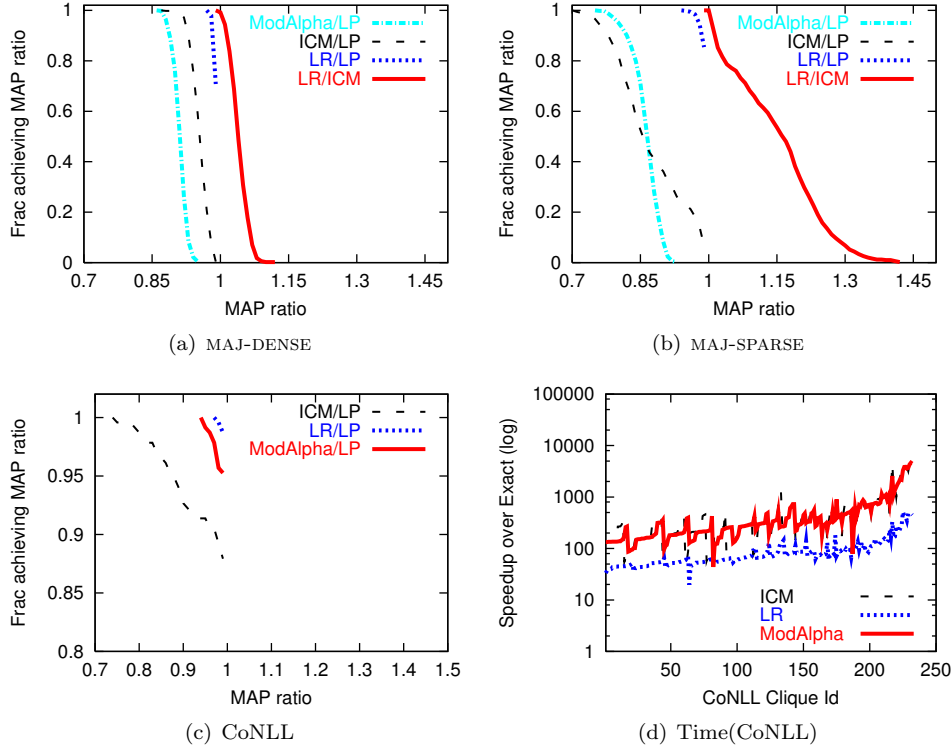


Figure 5: Comparing AlphaPass, ICM, Lagrangian Relaxation and Exact on MAJORITY potentials

because based on the experiments in [23] we expected this method to be faster. One reason could be that their experiments were on grid graphs whereas ours are on cliques.

7.1.2 Non-decomposable potentials

In this case, we cannot compare against the TRW-S or graph-cut based algorithms. Hence we compare with the ICM algorithm that has been popular in such scenarios [16]. We varied λ with increments of 0.02 in $[0.7, 1.1]$ and generated 500 cliques each from POTS, MAJ-DENSE, MAJ-SPARSE, ENTROPY, MAKESPAN and MAKESPAN2. We measure the ratio of MAP score of α -pass with ICM and for each ratio r we plot the fraction of cliques where α -pass returns a MAP that results in a ratio better than r . Figure 4(d) shows the results on all the potentials except majority. The curves for linear and square makespan lie totally to the right of $ratio = 1$, which is expected because α -pass will always return the optimal answers for those potentials. For Potts too, α -pass is better than ICM for almost all the cases. For entropy, α -pass was found to be significantly better than ICM in all the cases. The runtimes of ICM and α -pass were similar.

Majority Potentials

In Figures 5(a) and 5(b), we compare ICM, Lagrangian Relaxation (LR) and modified α -pass with the LP-based exact method on synthetic data. The dotted curves plot, for each MAP ratio r , the fraction of cliques on which ICM (or LR or modified α -pass) returns a MAP score better than r times the true MAP. The solid curve plots the fraction of cliques where LR returns a MAP score better than r times the ICM MAP. On MAJ-DENSE, both modified α -pass and ICM return a MAP score better than 0.85 of the true MAP, with ICM being slightly better. However, LR outperforms both of them, providing a MAP ratio always better than 0.97 and returning the true MAP in more than 70% of the cases. In MAJ-SPARSE too, LR dominates the other two algorithms, returning the true MAP in more than 80% of the cases, with a MAP ratio always better than 0.92. The solid curve in Figure 5(b) shows that on average, LR returns a MAP score 1.15 times that of ICM. Thus, LR performs much

better than its competitors across dense as well as sparse majority potentials.

The results on CoNLL dataset, whose W matrix is 85% sparse, are displayed in Figure 5(c). ICM, modified α -pass and LR return the true MAP in 87%, 95% and 99% of the cliques respectively, with the worst case MAP ratio of LR being 0.97 as opposed to 0.94 and 0.74 for modified α -pass and ICM respectively.

Figure 5(d) displays runtime ratios on all CoNLL cliques for all three inexact algorithms. ICM and modified α -pass are roughly 100-10000 times faster than the exact algorithm, while LR is roughly twice as expensive as ICM and modified α -pass. Thus, for practical majority potentials, LR and modified α -pass seem to quickly provide highly accurate solutions.

From now on, while doing the top-level message passing on the cluster graph, we shall use the α -pass and Lagrangian-relaxation based algorithms for computing messages from a clique, in the presence of Potts and MAJORITY potentials respectively.

7.2 Domain Adaptation

We now move on the generalized collective inference framework, and show that a good set of properties can help us in domain adaptation. We focus on the bibliographic task, where the aim is to adapt a sequential model across widely varying publications pages of authors. Our dataset consists of 433 bibliographic entries from the web-pages of 31 authors, hand-labeled with 14 labels such as Title, Author, Venue, Location and Year. Bibliographic entries across different authors differ in various aspects like label-ordering, missing labels, punctuation, HTML formatting and bibliographic style.

A fraction of 31 domains were used to train a baseline sequential model. The model was trained with the LARank algorithm of [3], using the BCE encoding for the labels. We used standard extraction features in a window around each token, along with label transition features [20].

For our collective framework, we use the following decomposable properties:

$$\begin{aligned}
 p_1(\mathbf{x}, \mathbf{y}) &= \text{First non-Other label in } \mathbf{y} \\
 p_2(\mathbf{x}, \mathbf{y}) &= \text{Token before the Title segment in } \mathbf{y} \\
 p_3(\mathbf{x}, \mathbf{y}) &= \text{First non-Other label after Title in } \mathbf{y} \\
 p_4(\mathbf{x}, \mathbf{y}) &= \text{First non-Other label after Venue in } \mathbf{y}
 \end{aligned}$$

Inside a domain, any one of the above properties will predominantly favor one value, e.g. p_3 might favor the value ‘Author’ in one domain, and ‘Date’ in another. Thus these properties encourage consistent labeling around the Title and Venue segments. We use Potts potential for each property, with $\lambda = 1$.

Some of these properties, e.g. p_3 , operate on non-adjacent labels, and thus are not Markovian. This can be easily rectified by making ‘Other’ an extension of its predecessor label, e.g. an ‘Other’ segment after ‘Title’ can be relabeled as ‘After-Title’.

The performance results of the collective model with the above properties versus the baseline model are presented in Table 3. For the test domains, we report token-F1 of the important labels — Title, Author and Venue. The accuracies are averaged over five trials. The collective model leads to upto 25% reduction in the test error for Venue and Title, labels for which we had defined related properties. The gain is statistically significant ($p < 0.05$). The improvement is more prominent when only a few domains are available for training. Figure 6 shows the error reduction on individual test domains for one particular split when five domains were used for training and 26 for testing. The errors are computed from the combined token F1 scores of Title, Venue and Author. For some domains the errors are reduced by more than 50%. Collective inference increases errors in only two domains.

Finally, we mention that for this task, applying the classical collective inference setup with cliques over repeated occurrences of words leads to very minor gains. In this context, the generalized collective inference framework is indeed a much more accurate mechanism for joint labeling.

7.3 Collective Labeling of Repeated Words

We now establish that even for simple collective inference setups without any multi-clique properties, message passing on the cluster graph (abbreviated as CI) is a better option. We consider information extraction over

Train %	Title		Venue		Author	
	Base	CI	Base	CI	Base	CI
5	70.7	74.8	58.8	62.5	74.1	74.3
10	78.0	82.1	69.2	72.2	75.6	75.9
20	85.8	88.6	76.7	78.9	80.7	80.7
30	91.7	93.0	81.5	82.6	87.7	88.0
50	92.3	94.2	83.5	84.5	89.4	90.0

Table 3: Token-F1 of the Collective and Base Models on the Domain Adaptation Task

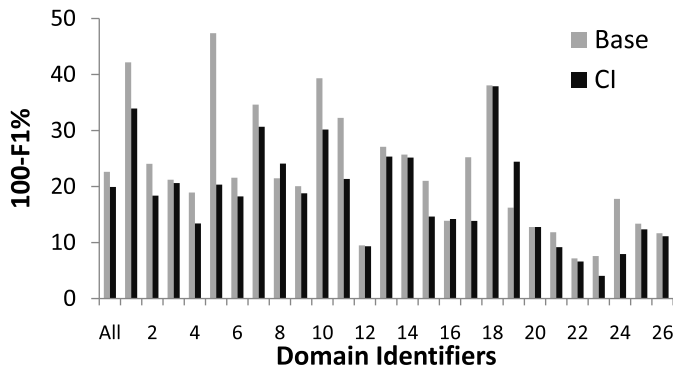


Figure 6: Per-domain error for the base and collective inference (CI) model

text records, and define cliques over multiple occurrences of words. We create two versions of the experiment — with Potts and MAJORITY potentials on the cliques respectively.

Since the Potts potential is decomposable over the clique edges, we compare CI against the TRW-S algorithm of [13] which is the state of the art algorithm for belief propagation. We compare the MAJORITY potential version against the stacking approach of [15].

We report results on three datasets — the Address dataset consisting of roughly 400 non-US postal addresses, the Cora dataset [18] containing 500 bibliographic records, and the CoNLL’03 dataset. The training splits were 30%, 10% and 100% respectively for the three datasets, and the parameter λ for Potts was set to 0.2, 1 and 0.05. The MAJORITY parameter W was learnt generatively through label co-occurrence statistics in cliques seen in the training data.

Table 4 reports the combined token-F1 over all labels except ‘Other’. Unless specified, all the approaches post statistically significant gains over the base model. For MAJORITY potentials, CI is superior to the stacking based approach. For the Potts version, there is no clear winner as TRW-S achieves F1 slightly better or close to those for CI. But collective inference with MAJORITY potentials is more accurate than with Potts.

Exploring Potts potentials further, we present Figure 7, where we plot the accuracy of the two methods versus the number of iterations. CI achieves its best accuracy after just one round, whereas TRW-S takes around 20 iterations. In terms of clock time, an iteration of TRW-S cost ~ 3.2 s for CORA, and that of CI cost 3s, so CI is roughly an order of magnitude faster than TRW-S for the same accuracy levels. The comparison was similar for the Address dataset.

Hence the CI approach is applicable for all symmetric potentials, and exploits their form to get higher accuracies faster than other methods.

Potential	Model	Address	Cora	CoNLL
	Base	81.5	88.9	87.0
Potts	CI	81.9	89.7	88.8
	TRW-S	81.9	89.7	-
MAJORITY	CI	82.2	89.6	88.8
	Stacking	81.7*	87.5↓	87.8

Table 4: Token F1 scores of various approaches on collective labeling with repeated words. Results averaged over five trials for Address and Cora. A '*' denotes statistically insignificant difference ($p > 0.05$), ↓ means statistically significant loss.

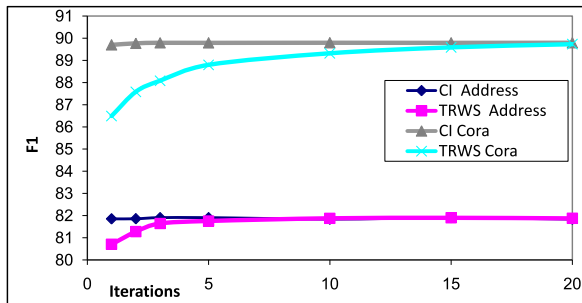


Figure 7: Accuracy with iterations for CI vs TRW-S on Cora and Address.

8 Conclusions and Future Work

We proposed a generalized collective inference framework based on decomposable properties and symmetric potential functions to maintain conformity in the labeling of multiple MRFs. We perform joint MAP inference using a cluster graph that defines special separator variables based on property values. The messages inside MRF clusters were modified to make them property-aware. Special combinatorial algorithms were used at the property cliques to compute outgoing messages.

We demonstrated the effectiveness of the framework by applying it on a domain adaptation task with a rich set of properties. We also established that message passing on the cluster graph is an effective solution vis a vis cluster-oblivious approaches based on ordinary belief propagation.

Algorithmically, we presented potential-specific combinatorial algorithms for inference in a clique. We gave a Lagrangian relaxation method for generating messages from a clique with majority potential. This algorithm is two orders of magnitude faster than an exact algorithm and more accurate than other approximate approaches. We also presented the α -pass algorithm for Potts potentials, which enjoys a tight approximation guarantee of $\frac{13}{15}$. This algorithm is sub-quadratic in the clique size. We showed that α -pass is faster and more accurate than alternatives such as TRW-S and graph-cuts.

Future directions

We wish to automate the selection of important decomposable associative properties. Another issue is the domain-adaptive training of the property parameters (e.g. λ for Potts). Joint training of these parameters with the baseline model would require expensive calls to the collective inference algorithm at each step, so a cheaper alternative has to be investigated.

Next, our property clusters are presently defined as cliques with symmetric potentials, which have limited expressive power. So we are interested in looking at dense weighted subgraphs instead of cliques, thus modeling that not all vertex-pairs have equal associativity.

Finally, we wish to seek more applications for collective inference, and deploy collective inference on a large scale. Although our cluster message passing based solution is distributed and inherently parallelizable, the clique participants might lie on different physical machines. This, and some other interesting scaling issues will crop up as we try to run collective inference on a web scale.

References

- [1] David Blei, Drew Bagnell, and Andrew McCallum. Learning with scope, with application to information extraction and classification. In *Conference on Uncertainty in Artificial Intelligence (UAI)*, 2002.
- [2] J. Blitzer, R. McDonald, and F. Pereira. Domain Adaptation with Structural Correspondence Learning. In *Proceedings of the Empirical Methods in Natural Language Processing (EMNLP)*, 2006.
- [3] Antoine Bordes, Léon Bottou, Patrick Gallinari, and Jason Weston. Solving multiclass support vector machines with larank. In *ICML*, pages 89–96, 2007.
- [4] Y. Boykov and V. Kolmogorov. An experimental comparison of min-cut/max-flow algorithms for energy minimization in vision. In *In IEEE Transactions on Pattern Analysis and Machine Intelligence (PAMI)*, volume 26, no. 9, pages 1124–1137, 2004.
- [5] Yuri Boykov, Olga Veksler, and Ramin Zabih. Fast approximate energy minimization via graph cuts. *IEEE Trans. Pattern Anal. Mach. Intell.*, 23(11):1222–1239, 2001.
- [6] Razvan Bunescu and Raymond J. Mooney. Collective information extraction with relational markov networks. In *Proceedings of the 42nd Annual Meeting of the Association for Computational Linguistics*, pages 439–446, 2004.
- [7] Soumen Chakrabarti, Byron Dom, and Piotr Indyk. Enhanced hypertext categorization using hyperlinks. *SIGMOD Rec.*, 27(2):307–318, 1998.
- [8] J. Duchi, D. Tarlow, G. Elidan, and D. Koller. Using combinatorial optimization within max-product belief propagation. In *Advances in Neural Information Processing Systems (NIPS 2006)*, 2007.
- [9] Jenny Rose Finkel, Trond Grenager, and Christopher D. Manning. Incorporating non-local information into information extraction systems by gibbs sampling. In *ACL*, 2005.
- [10] Rahul Gupta, Ajit A. Diwan, and Sunita Sarawagi. Efficient inference with cardinality-based clique potentials. In *Proceedings of the 24th International Conference on Machine Learning (ICML), USA*, 2007.
- [11] Berhanu Guta. *Subgradient optimization methods in integer programming with an application to a radiation therapy problem*. PhD thesis, Universität Kaiserslautern, 2003.
- [12] Jon Kleinberg and Eva Tardos. Approximation algorithms for classification problems with pairwise relationships: metric labeling and markov random fields. *J. ACM*, 49(5):616–639, 2002.
- [13] Vladimir Kolmogorov. Convergent tree-reweighted message passing for energy minimization. Technical Report MSR-TR-2004-90, Microsoft Research (MSR), September 2004.
- [14] Vladimir Kolmogorov and Ramin Zabih. What energy functions can be minimized via graph cuts. *IEEE Transactions on Pattern Analysis and Machine Intelligence*, 26, 2004.
- [15] Vijay Krishnan and Christopher D. Manning. An effective two-stage model for exploiting non-local dependencies in named entity recognition. In *ACL-COLING*, 2006.
- [16] Qing Lu and Lise Getoor. Link-based classification. In *Machine Learning, Proceedings of the Twentieth International Conference (ICML 2003), August 21-24, 2003, Washington, DC, USA*, pages 496–503, 2003.
- [17] Gideon Mann and Andrew McCallum. Simple, robust, scalable semi-supervised learning via expectation regularization. In *International Conference on Machine Learning (ICML)*, 2007.

- [18] Andrew McCallum, Kamal Nigam, Jason Reed, Jason Rennie, and Kristie Seymore. Cora: Computer science research paper search engine. <http://cora.whizbang.com/>, 2000.
- [19] C.H. Papadimitriou and K. Steiglitz. *Combinatorial Optimization: Algorithms and Complexity*, chapter 11, pages 247–254. Prentice Hall, Englewood Cliffs, NJ., 1982.
- [20] Fuchun Peng and Andrew McCallum. Accurate information extraction from research papers using conditional random fields. In *HLT-NAACL*, pages 329–336, 2004.
- [21] Pradeep Ravikumar and John Lafferty. Quadratic programming relaxations for metric labeling and markov random field map estimation. In *ICML*, 2006.
- [22] Charles Sutton and Andrew McCallum. Collective segmentation and labeling of distant entities in information extraction. Technical Report TR # 04-49, University of Massachusetts, July 2004. Presented at ICML Workshop on Statistical Relational Learning and Its Connections to Other Fields.
- [23] R. Szeliski, R. Zabih, D. Scharstein, O. Veksler, V. Kolmogorov, A. Agarwala, M. Tappen, and C. Rother. A comparative study of energy minimization methods for markov random fields. In *In Ninth European Conference on Computer Vision (ECCV 2006)*, volume 2, pages 16–29, 2006.
- [24] B. Taskar, P. Abbeel, and D. Koller. Discriminative probabilistic models for relational data. In *Eighteenth Conference on Uncertainty in Artificial Intelligence (UAI02), Edmonton, Canada*, 2002.

